Hydrologic Processes and Radionuclide Distribution in a Cavity and Chimney Produced by the Cannikin Nuclear Explosion, Amchitka Island, Alaska

By HANS C. CLAASSEN

HYDROLOGY OF NUCLEAR TEST SITES

GEOLOGICAL SURVEY PROFESSIONAL PAPER 712-D

Prepared on behalf of the
U.S. Energy Research and Development Administration

UNITED STATES GOVERNMENT PRINTING OFFICE, WASHINGTON : 1978

CONTENTS

ILLUSTRATIONS

TABLES

HYDROLOGIC PROCESSES AND RADIONUCLIDE DISTRIBUTION IN A CAVITY AND CHIMNEY PRODUCED BY THE CANNIKIN NUCLEAR EXPLOSION, AMCHITKA ISLAND, ALASKA

By HANS C. CLAASSEN

ABSTRACT

An analysis of hydraulic, chemical, and radiochemical data obtained in the vicinity of the site of a nuclear explosion (code-named Cannikin, 1971), on Amchitka Island, Alaska, was undertaken to describe the hydrologic processes associated with the saturation of subsurface void space produced by the explosion. Immediately after detonation of the explosive, a subsurface cavity was created surrounding the explosion point. This cavity soon was partly filled by collapse of overburden, producing void volume in a rubble chimney extending to land surface and forming a surface-collapse sink. Surface and ground water immediately began filling the chimney but was excluded for a time from the cavity by the presence of steam. When the steam condensed, the accumulated water in the chimney flowed into the cavity region, picking up and depositing radioactive materials along its path. Refilling of the chimney voids then resumed and was nearly complete about 260 days after the explosion. The hydraulic properties of identified aquifers intersecting the chimney were used with estimates of surface-water inflow, chimney dimensions, and the measured water-level rise in the chimney to estimate the distribution of explosion-created porosity in the chimney, which ranged from about 10 percent near the bottom to 4 percent near the top.

Chemical and radiochemical analyses of water from the cavity resulted in identification of three aqueous phases — ground water, surface water, and condensed steam. Although most water samples represented mixtures of these phases, they contained radioactivity representative of all radioactivity produced by the explosion. Sorption of radioactivity on particulate matter was evident, more than 10,000 times as much activity being found on solids as in solution; however, no selectivity for specific isotopes was observed, and sorption equilibrium had not been reached 400 days after the explosion.

Although large amounts of heat were released by the Cannikin explosion, approximately 90 percent of this heat was absorbed by rock and water that fell into the cavity. As heat in the cavity dissipated to the surroundings, additional voids were created by cooling of the rocks that had fallen into the cavity; this new space in part accounted for the continued water flow into the cavity observed after chimney filling was virtually complete. The occurrence of zones of low hydraulic conductivity may also have contributed to the delay in filling the cavity.

INTRODUCTION

A nuclear device, code-named Cannikin, was detonated November 6, 1971, 5875 ft (1790 m) below land surface on Amchitka Island, Alaska, as part of the weapons-testing program of the U.S. Energy Research and Development Administration (formerly the U.S. Atomic Energy Commission). For details concerning the Cannikin experiment, see Merritt (1973). After detonation of the device, a reentry hole was drilled into the subsurface cavity formed by the explosion. One of the purposes of the reentry hole was to provide data for a better understanding of the postdetonation hydrologic processes occurring in a nuclear-explosion-produced cavity and chimney in volcanic rocks.

In addition to acquiring hydrologic information, the postdetonation studies were intended to provide data on radionuclide distribution in the cavity and to allow estimation of radionuclide concentrations in cavity water which would be useful for improving predictions of possible contamination hazards associated with underground nuclear testing in a saturated zone. Unfortunately, conditions under which samples were obtained for analysis were less than ideal, and the stated goals were not reached in every respect; nevertheless, valuable data useful for understanding the movement and chemical behavior of radionuclides were obtained.

Amchitka Island is the southernmost and largest island of the Rat Island group, part of a chain of islands extending from the Alaskan Peninsula and forming the southern boundary of the Bering Sea (fig. 1). The humid climate contributes to a nearly saturated subsurface environment, composed entirely of volcanic rocks,

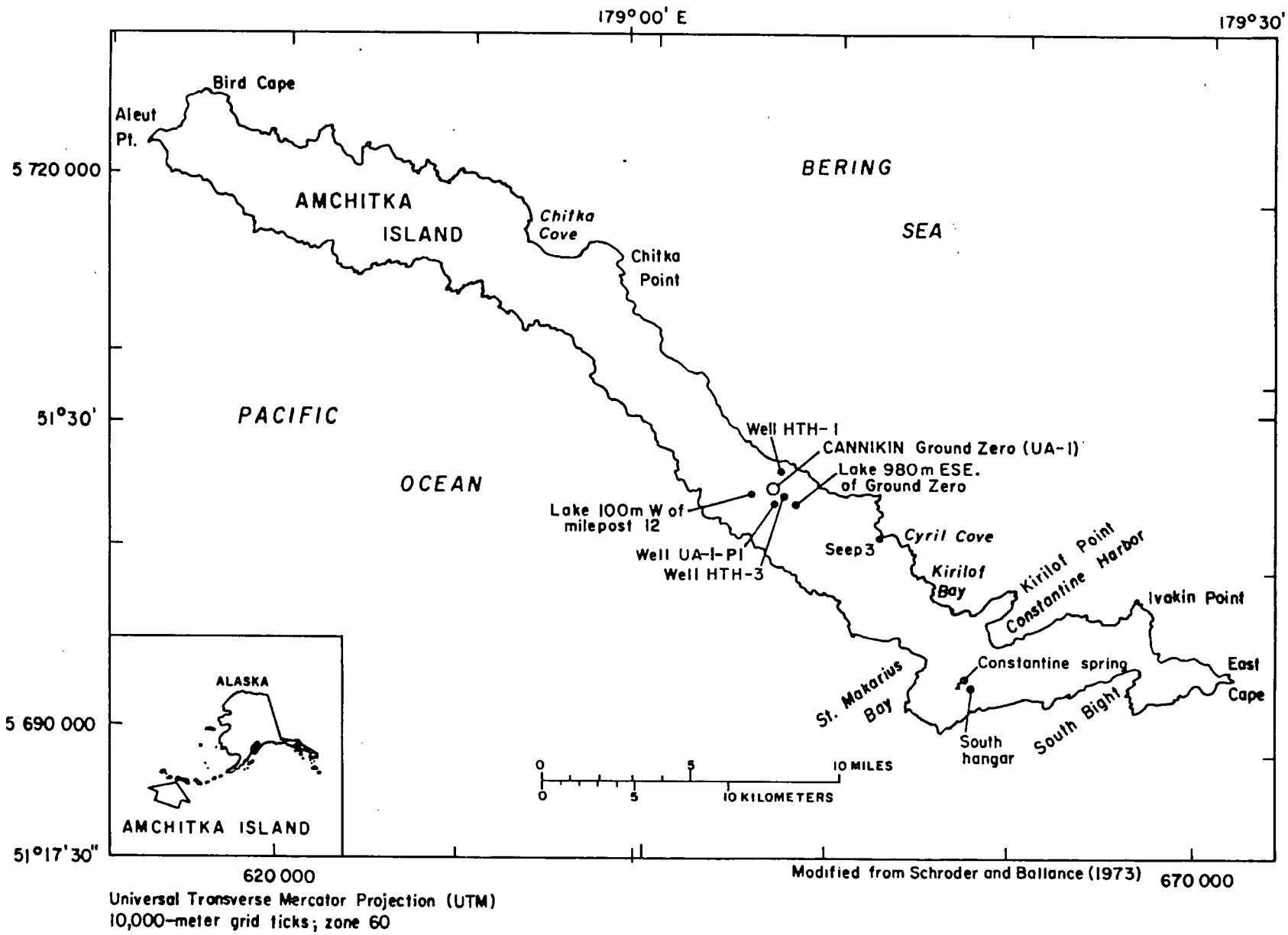

FIGURE 1. — Location of selected sampling sites, Amchitka Island, Alaska.

which are gently southeastward dipping andesite lava flows and breccias and basalts (Carr and Quinlivan, 1969). Both the surface hydrologic system in the vicinity of the site of Cannikin SGZ (surface ground-zero) (W. C. Ballance, written commun., 1975) and the subsurface system have been investigated in detail (W. W. Dudley, Jr., written commun., 1971; Ballance, 1970, 1972). Both perennial and ephemeral lakes and streams are common on Amchitka, but the most significant surface hydrologic feature in the vicinity of Cannikin SGZ is White Alice Creek. After detonation of the device (zero time), another significant feature appeared: Cannikin Lake (fig. 2).

The undisturbed subsurface hydrologic system included four main zones of different horizontal hydraulic conductivity. Hydraulic and water-quality data from the subsurface environment around the Cannikin site indicated that a low vertical hydraulic conductivity was also present prior to the detonation of the nuclear device. Little vertical flow was indicated, as there was little change in hydraulic potential with depth below the uppermost zone of hydraulic conductivity (Ballance, 1972) and only gradual increases in salinity with depth (Fenske, 1972). Whether this is due to low vertical hydraulic conductivity or merely a consequence of a low vertical hydraulic gradient is not certain, but the nearly horizontal bedding and differences in horizontal hydraulic conductivities of the volcanic rocks comprising the geologic framework around the Cannikin site favor the former explanation.

The discussion that follows begins with the hydrologic processes believed to have occurred after detonation and then moves to an examination of water-quality changes in both stable and radioactive species. Care has been taken to place qualifications on the data obtained and to reach only those conclusions that seem warranted in light of the indicated constraints.

HYDROLOGIC PROCESSES IN THE CANNIKIN CAVITY AND CHIMNEY

Description of the hydrologic processes occurring in the cavity and chimney regions was an area of major importance in the investigation summarized by this report. The approach was to postulate a series of events and processes that fits the existing data (within the limits of accuracy of those data), both spatially and temporally. It was not certain at the outset that a unique solution to the problem would be obtained; however, it appears that for a given set of values for certain key parameters, a specific series of events must be postulated. A description of these events follows.

EVENTS OCCURRING PRIOR TO AND FOLLOWING CONDENSATION OF STEAM IN THE CANNIKIN CAVITY

Upon underground detonation of a nuclear device designed for containment, the rock melts and vaporizes; an underground cavity is formed; and shattering of rock surrounding the cavity occurs in a region about two cavity radii from the emplacement point of the device (WP). The region of shattered rock is called the shock zone. (See, for example, Higgins and Butkovich, 1967.)

The cross sections of the Cannikin cavity and chimney shown on plate 1 are in the vertical plane $A-A'$, whose intersection with the land surface is shown in figure 2. The location of the drill hole was determined by directional logging and is projected onto the plane $A-A'$.

The series of cross sections on plate 1 depict conditions at 13 points in time during the history of the Cannikin site, starting immediately (1 minute) after detonation and continuing until the site was abandoned.

Although the sequence of events depicted on plate 1 would be similar for any underground nuclear explosion in a saturated medium, the timing and quantitative aspects of the events in the sequence are dependent on the hydraulic and physical properties of the medium. Thus, values for certain key parameters must be postulated in order to produce the sequence of events depicted on plate 1.

One of the key parameters affecting the hydraulic history of a nuclear explosion cavity is the day on which steam begins to condense in the cavity. The data presented and the interpretations developed in following section of this report are consistent with the hypothesis that steam in the hot cavity region began to condense 60 days after zero time. The reasons for selection of this value for the day of condensation will be developed in the succeeding discussion. The actual dimensions of the cavity are classified national-security information. For purposes of scaling on plate 1 and of calculating derived values, such as the water level in the chimney, the cavity radius is chosen as $R_{rc} = 1.34$; this is one of a range of cavity radii considered in subsequent sections of this report and is 34 percent greater than the smallest cavity considered, which was arbitrarily assigned to a value $R_{rc} = 1.00$.

Plate 1*A* shows the hydrologic system about 1 minute after detonation (zero time). The cavity has reached its maximum size and is filled mainly with steam released from the melted rock. This steam is at high temperature, and the pressure rapidly approaches a value approximating lithostatic pressure. Some raising of the

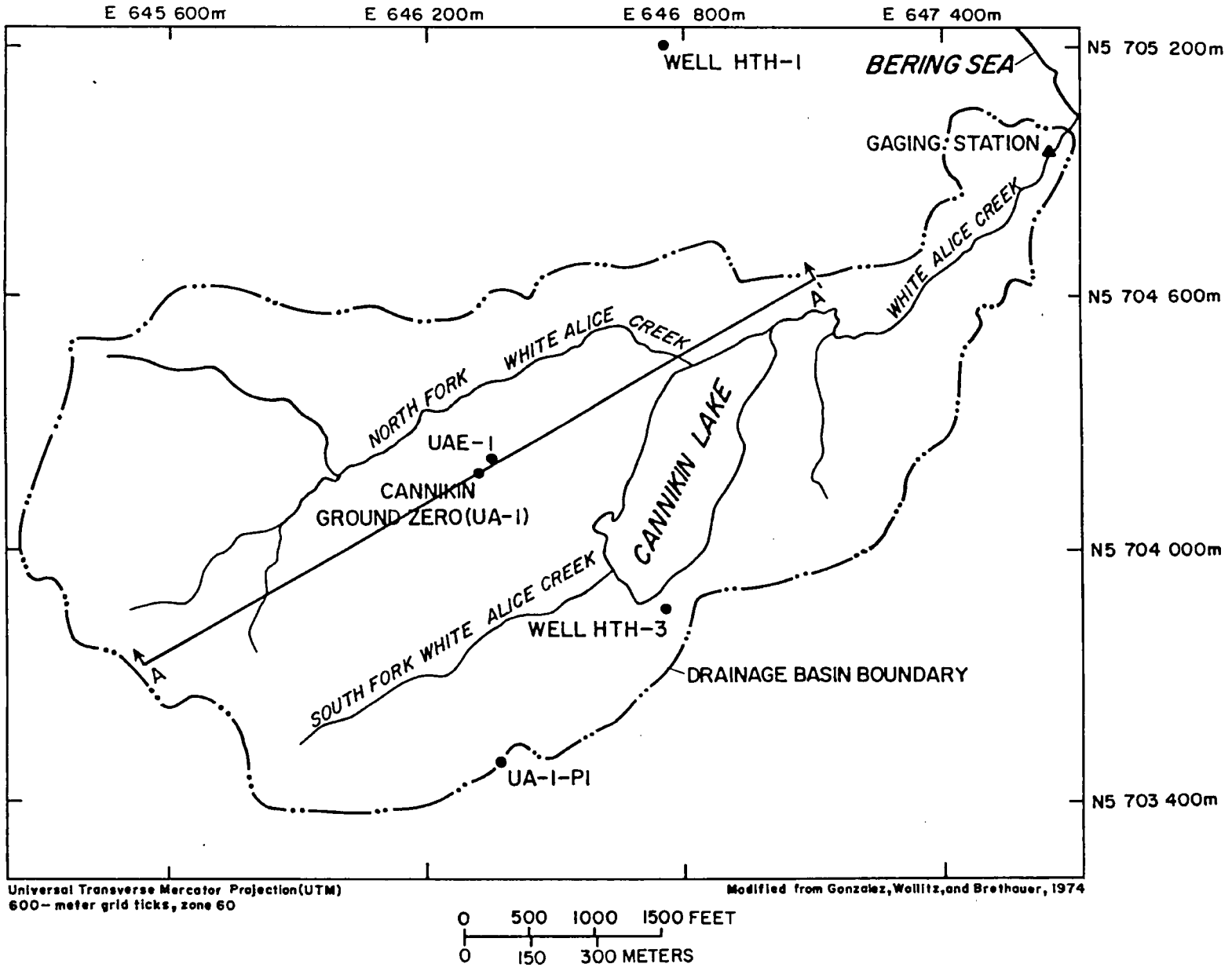

FIGURE 2. — Intersection *A*–*A'* of projection plane with land surface, White Alice Creek drainage basin and location of selected sites in the vicinity of Cannikin ground zero, Amchitka Island, Alaska.

ground surface has occurred, and water in lakes and streams has been thrown into the air.

By day 2 since zero time (pl. 1*B*), the pressure in the cavity has dropped sufficiently to allow overburden material to fall into the cavity, creating a rubble chimney between the cavity and the surface and a collapse sink at the surface. The collapse sink was surveyed by Holmes and Narver, Inc., and its volume determined by comparison of present with previous topography. See Merritt (1973) and Morris (1973). The collapse sink intercepted nearly all surface drainage in the White Alice Creek basin, and the formation of the chimney allowed inflow from the four aquifers indicated by increasing vertical conductivity in the chimney. It is hypothesized that flow into the cavity is retarded at this stage by the presence of a region containing water as both liquid and vapor. The vapor tends to rise and to be condensed by cooler, saturated rock above; the liquid front will tend to move downward in response to increasing head (remember that water is continually accumulating above this liquid-vapor interface in the chimney from both surface and subsurface sources), but this water will encounter rock and water vapor at higher temperature, resulting in further vaporization. Mass transfer of water into the cavity region is thus retarded. Another mechanism that may contribute to flow retardation is the lowered conductivity to water in the two-phase region, if conductivity relationships are similar to those observed in natural-gas reservoirs. (See, for example, Pirson, 1958.) These systems exhibit conductivity minimums under two-phase conditions; conductivities to the liquid phase have been observed that are more than one order of magnitude lower than those for either liquid alone or gas alone.

When temperatures in the cavity region have been sufficiently lowered, downward-percolating water no longer vaporizes, and the water front can move downward under single-phase flow conditions.

The above hypothesis is reinforced by a comparison of diagrams on plate 1 which show the declining water levels measured in the drill stem on days 60, 67, 70, 90 and 100 since zero time. Therefore, the day on which condensation began was assumed to be day 60. Conditions postulated for day 60 are shown on plate 1*C*. The reentry hole (UA–1–P1) has penetrated the chimney, and the composite water level measured in the drill stem is indicated. Using methods discussed later in this report to calculate inflow to the chimney, assuming retardation of flow into the cavity region, the calculated water level in the chimney on day 60 is also shown on plate 1*C*. If condensation in the cavity now occurs and if the vertical hydraulic conductivity throughout the bulk of the chimney is fairly high (at least as high as the horizontal hydraulic conductivity of the contributing aquifers — about 0.3 to 3 ft/d or 0.1 to 1 m/d), the accumulated water begins to flow into the cavity. By day 70 (pl. 1*E*) the drill hole has advanced about 1000 ft (330 m), and the composite water level measured in the drill stem has dropped about 2600 ft (790 m). On day 100 (pl. 1*G*) the reentry hole is near completion, and the composite water level in the drill stem is lower than on day 70. Assuming that the composite water level in the drill stem is representative and indicative of near-saturated conditions in the chimney, a significant change in chimney conditions has occurred between days 60 and 100, which corroborates the hypothesis of flow retardation prior to condensation.

On day 106 (pl. 1*H*) the reentry hole is completed, logged, and perforated, the water level having declined approximately an additional 400 ft (120 m) since day 100. The pressure indicated by the water level in the drill stem at the perforated interval A is primarily the sum of the water-vapor pressure at the prevailing temperature of the measuring point plus the true hydraulic head.

Figure 3 shows an approximate temperature history of the cavity region. Unfortunately, only a few temperature measurements were made, and some of these were discarded as not valid because of hole condi-

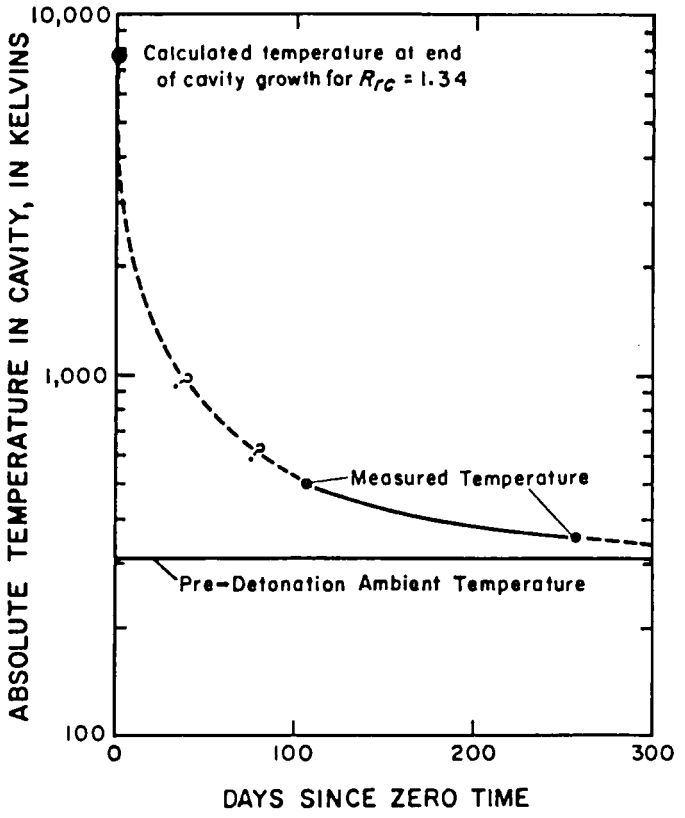

FIGURE 3. — Temperature history of the Cannikin cavity.

tions — for example, as a result of the addition of water to the drill stem. The two temperature measurements plotted in figure 3 are thought to be representative of conditions in the vicinity of the pressure measuring point, interval A (pl. 1*H*).

Because water-level measurements made in the drill stem represented total pressure in the cavity (that is, steam pressure plus head of water in chimney above the cavity), they were corrected by subtracting the water-vapor pressure to arrive at the actual water level in the chimney. Changes in water-vapor pressure with time were determined using the temperature curve in figure 3. The resulting hydraulic heads (corrected water levels) are plotted in figure 4, which shows the true rise in water level in the chimney in relation to the various contributing aquifers. An analysis of these data to determine the porosity (created by the nuclear explosion) distribution in the chimney is presented later in this report.

By about day 245 (pl. 1*I*), there is a cessation of water-level rise in the drill stem, indicating plugging of the perforations. Surging of the water in the hole during additional perforating and sampling operations on or about day 264 caused an abrupt rise in water level of about 220 ft (67 m).

The next significant event in chimney-infill history is the filling of Cannikin Lake, which began about day 288 (pl. 1*K*) and ended about day 383 (pl. 1*L*), as evidenced by resumption of normal flow in White Alice Creek.

Plate 1*M* illustrates conditions in the chimney region on day 543 just before abandonment and plugging of the reentry hole in May 1973. The water level in the chimney has changed only slightly since day 383 and is still below the level prior to Cannikin. What, then, can be predicted about the behavior of the chimney flow system when steady-state has been reached? Among the various contributing aquifers there is a difference in potential of as much as 11 ft (3.3 m) (Ballance, 1972, p. 30), and, because on day 543 the water level in the chimney was still 23 ft (7.0 m) below the potential of even the lowest of these, it can further be asserted that no inter-aquifer flow was taking place. It would be reasonable to predict that when chimney water levels rise another 23 ft (7.0 m), flow from aquifers with higher-potential to aquifers with lower potential will begin. On the basis of the rate of chimney-water-level rise measured from days 513 to 543, the new flow pattern would commence on about day 715. The aquifers of lowest measured potential (Ballance, 1970, 1972) are in the cavity region, but they are the zones, although classified as aquifers in this report, that have the lowest transmissivities. This, coupled with the small potential differences expected (less than 11 ft or 3.3 m) should result in minimal flow. One additional factor needs to be considered, however. Since creation of a rubble chimney has presumably greatly increased the vertical hydraulic conductivity over that existing in the undisturbed system, the effect of surface water contribution to the chimney must be assessed. Temperature logs and spinner surveys (surveys to indicate direction and amount of water flowing vertically in an open or cased hole) made in the drill stem at various times indicate that the reentry hole is acting as a recharge path from near ground surface to the cavity region. The ground surface is 163 ft (50 m) above the static water level of the aquifer with the highest potential considered (aquifer I); thus, the effective hydraulic potential between the ground surface and the aquifers in the cavity region may be as much as 163 ft (50 m) greater than the potential differences among the aquifers themselves. The ultimate effect of this modified hydrologic system on radionuclide transport cannot be estimated, as much of the flow in the system may be diverted to aquifers above the zone of major radioactive contamination.

Significant downward flow from the uppermost perforations to at least below the lowermost perforations (perforations made in July 1972) was observed in the drill stem prior to and at the time of abandonment of the reentry hole. Since the aquifer head relationships were such that no such flow should occur, an explanation is warranted. Two explanations follow; whether either or both are correct cannot be determined with certainty. The first explanation is that the effective storage capacity of the cavity region increases as the water temperature decreases. For example, a decrease in absolute temperature of 1 K (at the approximate temperature of the cavity on day 260 of 360 K) results in a fractional decrease in water volume of 2×10^{-4} whereas the aquifer matrix undergoes an estimated decrease of about 4×10^{-5} (both values estimated from Hodgman, 1957). If a given amount of heat is transferred from a region of saturated higher porosity to a region of saturated lower porosity, as might occur from the water-filled cavity to the surrounding aquifer, a net increase in storage results in the region of higher porosity, and water flows toward that region.

The second possible explanation is that the cavity contains subregions of low-permeability void which are only slowly being saturated, relegating the assumption of complete saturation of the cavity and near-saturation of the chimney by day 260 to that of an approximation. The actual situation is most likely a combination of these two mechanisms, but their relative importance is not known.

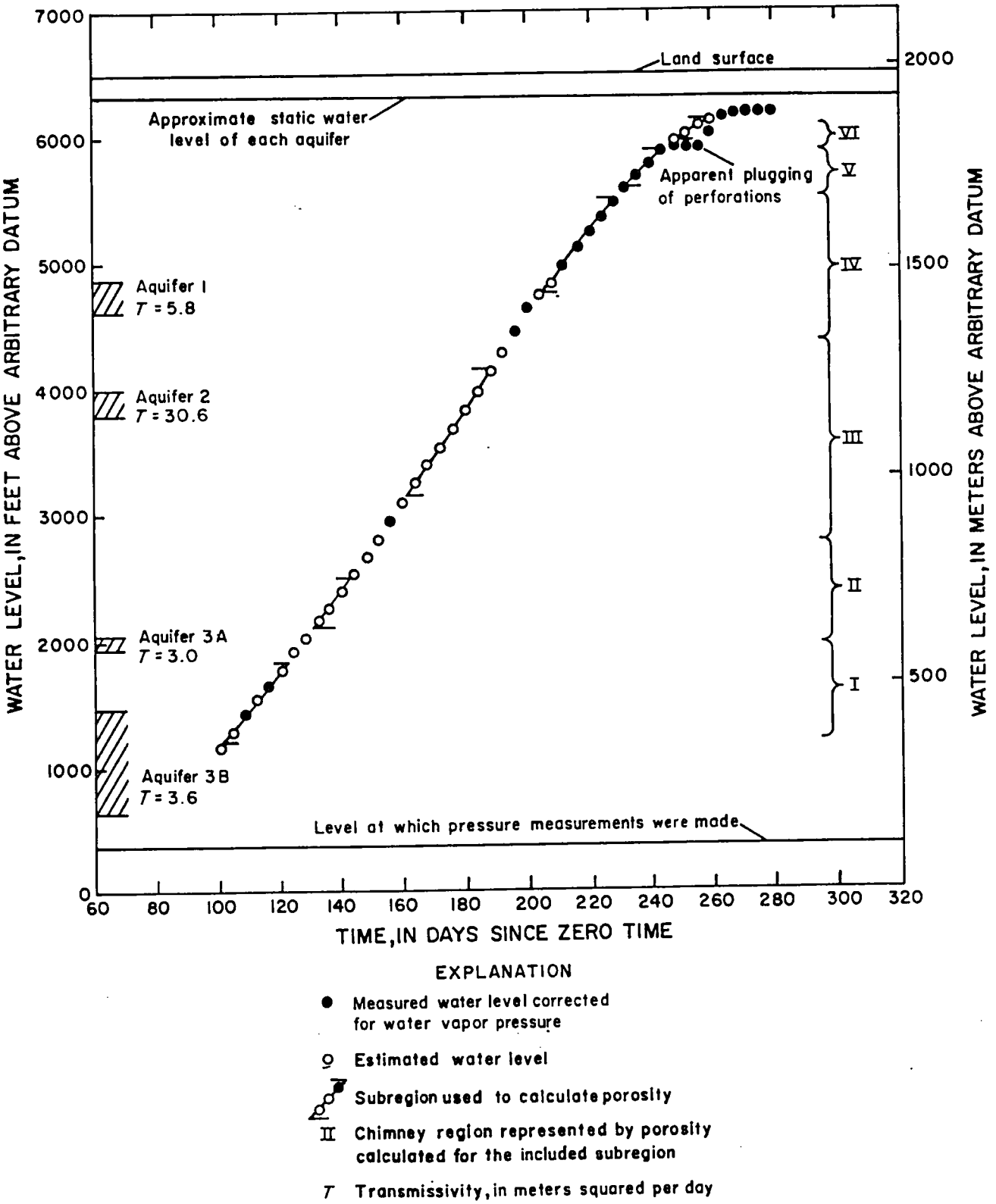

FIGURE 4. — Water-level history of the Cannikin chimney and its relation to aquifers and other regions of interest intersected by the cavity and chimney.

DETERMINATION OF THE DISTRIBUTION OF CHIMNEY POROSITY CREATED BY THE CANNIKIN EVENT

The vertical distribution of porosity in the rubble chimney created by the collapse of the subsurface explosion cavity is determined by the rate of rise of water level in the chimney. Required information includes the rate of inflow from all sources yielding water to the cavity and chimney, the dimensions of the chimney, and the variations in the rate of rise of true water level in the chimney.

Determination of the rate of inflow from all sources requires that the aquifer characteristics be known. Information on aquifer characteristics was obtained from hydraulic-test data published by Ballance (1970, 1972) and analyzed by W. W. Dudley, Jr. (written commun., 1970; table 1), to determine transmissivity, storage coefficient, porosity, and hydraulic conductivity. The bulk of the data is from UAE–1, a hole northeast of the emplacement hole UA–1 (fig. 2). Since time-dependent inflow from all contributing aquifers was desired, the total inflow time from $t = 0$ (zero time) to $t = 260$ days was broken up into discrete intervals of varying length, small time intervals near day zero and increasing in length as t approached day 260. For each of these time intervals a constant drawdown (the mean of the actual drawdown range during the time interval) for each aquifer was assumed, and the method of Hantush (1959), as modified by Dudley (1970), was used to compute inflow rates. In order to determine these inflows accurately, the effective radius of the chimney, R_{CH}, is required. For the assumed right-circular-cylinder configuration of the chimney, the cavity radius approximately equals the chimney radius. The *measured* radius of the cavity and related dimensions for the Cannikin event are classified information, so a range of values was chosen for computational purposes. See the section entitled "Calculation of Cavity Radius for the Cannikin Event" for calculations relating relative radii (R_{rc}) to absolute radii (R_c) using unclassified data. All these radii were related to the smallest chose ($R_{rc} = 1.00$) by a simple ratio; thus, $R_{rc} = 1.17$ indicate that this specified cavity radius is 1.17 times as large a the smallest one chosen for analysis.

So that a unique solution to the Cannikin hydrologi history can be obtained, the exact subsurface voi volume (V_{SUBSFC}) must be known. This volume i defined as the difference between the initial cavity voi prior to collapse ($V_C = {}^4/_3\pi R_c^3$, assuming sphericity) an the void expressed as a surface subsidence (V_{SINK}) Because measurements of cavity voids are classified only relative volumes are used in this report. (See "Calculation of Cavity Radius for the Cannikin Event' section for method of calculating R_c using publishec data.) It will be shown that a fairly wide range of values for R_c and V_C yield a rather narrow range of values for chimney porosities and result in porosity *distributions* which are virtually invariant.

An assumption made in the inflow analysis, which has been previously discussed, is that flow into the cavity region is severely retarded prior to steam condensation. Thus, infill is composed of two sequential events: initially, chimney filling progresses to day of condensation (D_C), the accumulated chimney infill then flowing into the cavity region; and secondly, chimney filling begins anew and continues smoothly until the chimney is nearly (95 percent) filled — chosen in this analysis arbitrarily as day 260. Because the total inflow to the system is dependent on the value chosen for the day of condensation as well as aquifer properties and chimney radius, a time-dependent matrix of values results for each set of chosen parameters. An example of the time variation of daily contributions from each aquifer (and surface water) and their summed contribution for $D_C = 60$ and $R_{rc} = 1.34$ is shown in figure 5.

Once a set of daily flows (such as in fig. 5) was determined for several paired values of R_{rc} and D_C, each was fitted to portions of the actual infill curve (fig. 4) to determine chimney porosity distribution as follows. The infill curve was broken up into subregions of approximately linear filling rate; these subregions are indicated by the straight-line segments superimposed on the infill curve of figure 4. Each segment is characterized by an initial (subscript i) and final (subscript f) value for both day (D_i, D_f) and water level (h_i, h_f). Associated with the interval D_i to D_f is a volume of water inflow (q_I) required to saturate the volume of chimney of porosity n represented by the water-level rise ($h_f - h_i$). Thus,

$$n = \frac{q_I}{\pi R_{CH}^2 (h_f - h_i)}$$

Each of the subregions were treated in this manner for each paired value of R_{rc} and D_C. The subregions were

TABLE 1. — *Summary of hydraulic data obtained in hole UAE–1, Amchitka Island, Alaska*

Interval tested distance above arbitrary subsurface datum (m)	Thickness of interval tested (m)	Transmissivity (m^2 /d)	Aquifer No.	Storage coefficient
1635.7–1559.0	76.7	5.8	1	1×10^{-4}
1363.8–1336.4	27.6	30	2	3×10^{-4}
1171.8–1153.5	18.3	.6		
766.3– 735.8	30.5	3.0	3A	6×10^{-4}
591.3– 542.5	48.8	.5	3B	6×10^{-4}
541.0– 480.9	60.1	.25		
479.1– 467.5	11.6	2.0		
476.7– 398.0	78.7	.52		
398.6– 338.2	60.4	.32		

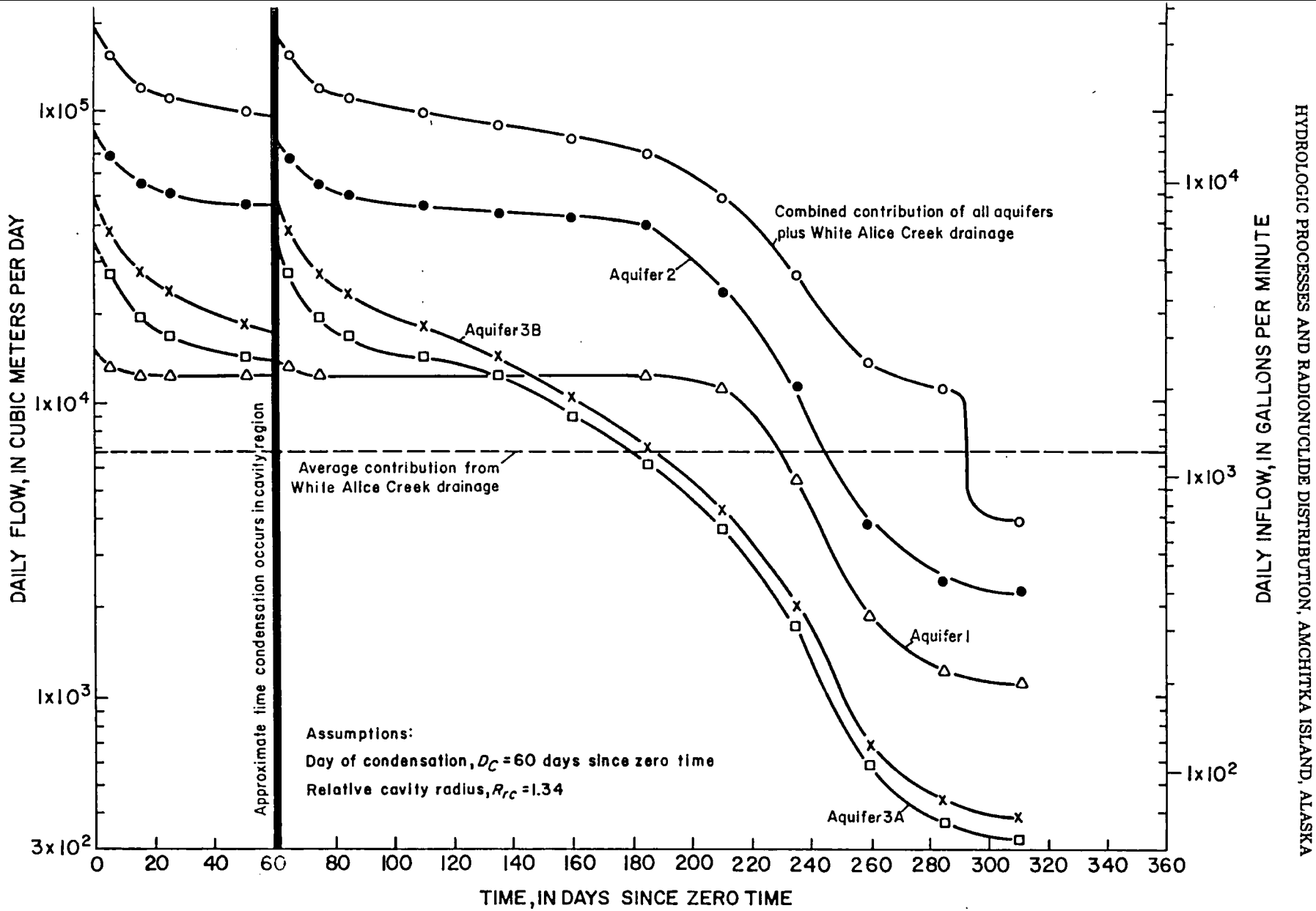

FIGURE 5. — Daily flow contribution to the Cannikin chimney from each aquifer and the White Alice Creek drainage and the combined contribution of all aquifers plus the White Alice Creek drainage.

then expanded slightly to the regions (indicated by Roman numerals in fig. 4) and the porosity value obtained for the subregion then applied to the entire region, to include the entire height of chimney represented by measured water levels. Various values for D_C were chosen for each of several R_{rc}'s and some of the results plotted in figure 6. Not all the calculated values are plotted, inasmuch as the effects of varying cavity size and day of condensation are well illustrated by using only some of the computed data. The greatest effect on absolute porosity is brought about by variations in cavity size and, consequently, chimney size; for example, an increase in subsurface void volume of 170 percent $R_{rc} = 1.00$ to $R_{rc} = 1.40$) results in a relative decrease in calculated overall porosity of about 45 percent throughout the chimney. The effect of an error in choice of D_C is slight; an error of 40 days produces an absolute error of only about 0.01 in the porosity at chimney top and bottom and a negligible error in chimney mid-region porosity estimates.

The total flow into the chimney must fill the available void volume — no more, no less. Figure 7 illustrates the effect of varying cavity size and day of condensation on the fraction of void filled by day 260. Day 260 has been arbitrarily chosen as representing completely filled conditions, even though only 95 percent of theoretically fillable chimney has been saturated as indicated by water-level data in figure 4. The value 1.0 on the ordinate represents a completely filled (by day 260) chimney. Referring to figure 5, note that shifting the day of condensation to smaller values (earlier times) would result in lower total flow to a chimney of given size; $R_{rc} = R_{CH} = 1.34$ in this example. In figure 7, for $R_{rc} = 1.00$, no D_C, day of steam condensation in the cavity, can be chosen which will generate little enough flow to do anything but overfill the available subsurface void in the allotted filling time. If the subsurface void volume is determined by assuming a spherical cavity (whose radius is determined by the measured radius of the lower hemisphere) and subtracting the sink volume, and if the aquifer characteristics and infill data that were used in making the calculations are correct, only irrational results are obtained. Uncertainties in both cavity geometry (the cavity may not be spherical, and the void produced may actually be greater than that calculated assuming sphericity) and in collapse-sink volume (surveying errors) produce uncertainty in any determination of the subsurface void, and prevent the condition of total inflow by day 260 (Q_I^{260}) equals V_{SUBSFC} from being met. This condition must be satisfied for an exact determination of the explosion-produced chimney porosity distribution. Pressure and temperature data prior to day 106, if available, would allow independent determination of day of condensa-

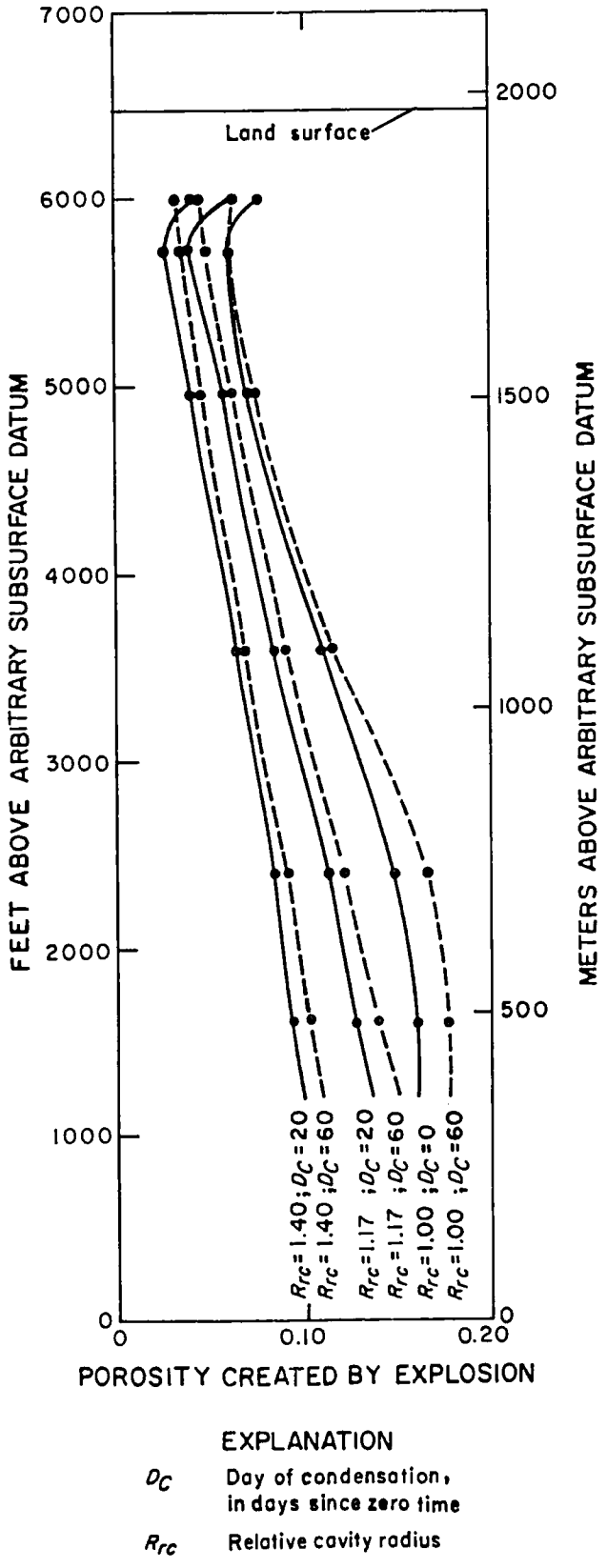

FIGURE 6. — Hypothetical porosity distribution in the Cannikin chimney for three cavity sizes and two days of condensation each.

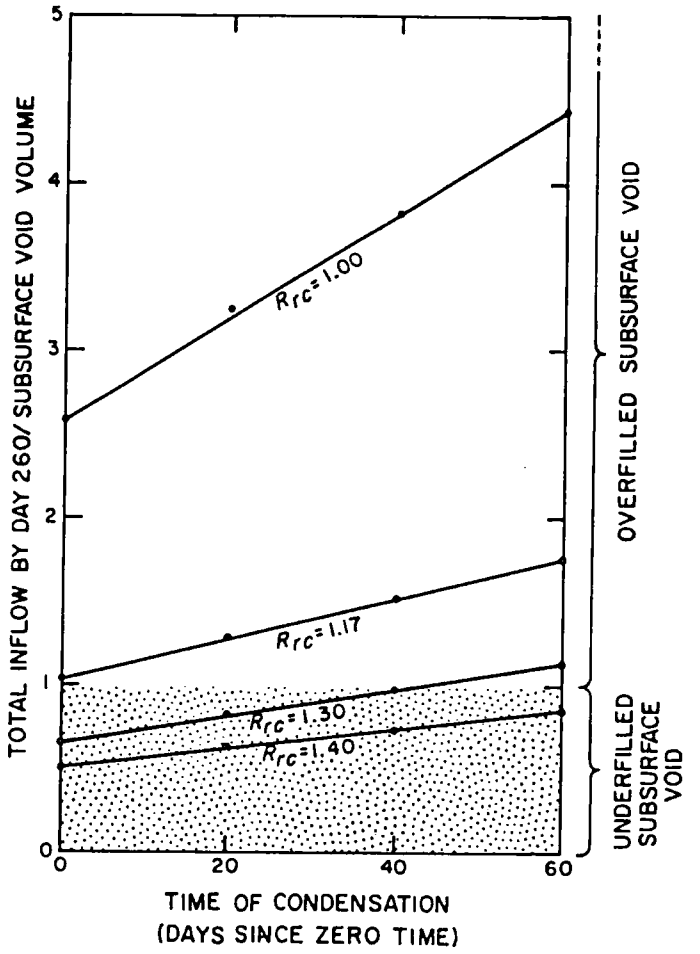

FIGURE 7. — Effect of cavity size and time of condensation on fraction of subsurface void volume filled by day 260.

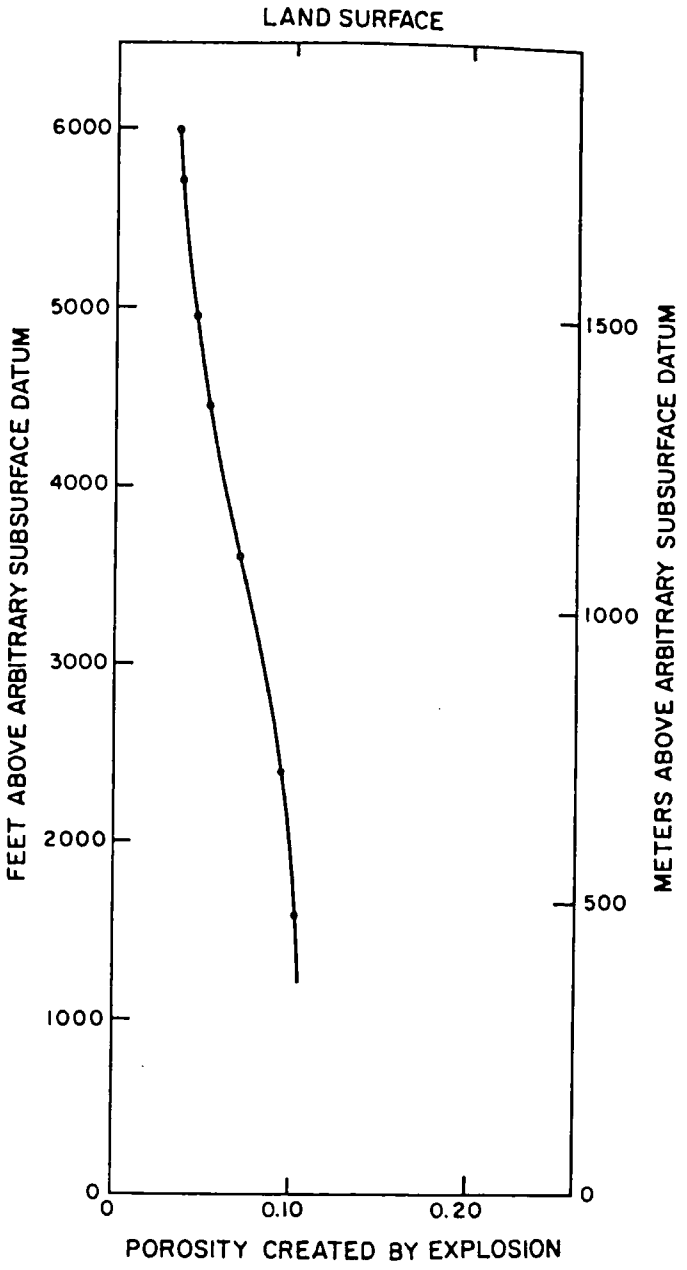

FIGURE 8. — Porosity distribution in the Cannikin chimney for $R_{rc} = 1.34$ and $D_C = 60$.

tion rather than reliance on inference ($D_C \simeq 60$) from water-level data as previously discussed. (See p. D5.)

On the assumption that the $D_C \simeq 60$ estimate is correct, interpolation between the curves $R_{rc} = 1.30$ and $R_{rc} = 1.40$ in figure 7 to obtain a curve which would intersect $Q_I^{260}/V_{SUBSFC} = 1$ at $D_C = 60$ yields an $R_{rc} \simeq 1.34$. Figure 8 shows the resultant chimney porosity distribution, about 10 percent near the bottom to about 4 percent near the top. This calculated porosity distribution is very different from that assumed by Fenske (1972) in his prediction of Cannikin chimney infill — 0 percent at the bottom, rising linearly to 14 percent at the top. In the only other published determination of rubble-chimney porosity, Garber (1971) reported a porosity range of about 7 percent near the bottom of the chimney to about 2 percent at a point about 200 ft (61 m) above the chimney bottom. The nuclear device was detonated at a point less than half the depth of Cannikin, in zeolitized tuff, and Garber's method of analysis consisted of comparing the volume of water removed during a pumping test with the observed interruption in water-level rise resulting from infill.

HEAT DISTRIBUTION IN THE CANNIKIN CAVITY

The heat generated by the approximately 5 megaton TNT-equivalent Cannikin explosion was calculated by the method of Heckman (1964) to be 5×10^{15} calories (cal). Assuming the heat to be distributed among the

various infill materials by day 100, estimates of heat capacity (Hodgman, 1957) were combined with published values for before-detonation rock bulk density and porosity (Lee and Gard, 1971) and the temperature from figure 3 to produce the following results for the system $R_{rc} = 1.34$ and $D_C = 60$.

1. Heat required to raise temperature of rock melted by explosion from ambient to temperature of cavity region on day 100, $\Delta H_1 = 7.1 \times 10^{14}$ cal.

2. Heat required to raise temperature of water contained in rock melted from ambient, $\Delta H_2 = 5.6 \times 10^{13}$ cal.

3. Heat required to raise temperature of water infill to cavity region (estimated) by day 100, $\Delta H_3 = 2.0 \times 10^{15}$ cal.

4. Heat required to raise temperature of saturated rock infill generated by collapse of shock zone above cavity into cavity, $\Delta H_4 = 2.5 \times 10^{15}$ cal.

Total heat required to raise cavity region contents to estimated conditions on day 100 is

$$\sum_{i=1}^{4} \Delta H_i = 5 \times 10^{15}.$$

The agreement with the amount of heat produced is probably fortuitous, inasmuch as fairly large errors are possible in all of the estimates and a 20 percent error would still be considered a good estimate; nevertheless, the implication that about 40 percent of the energy appears to be deposited in infilling water (ΔH_3) and 50 percent in collapsing saturated rock (ΔH_4) is probably valid. The remaining 10 percent is found in ΔH_1 and ΔH_2 above.

Note that no caloric term has been included to represent conduction of heat away from the cavity region. Preliminary calculations made by the author indicate that such a conduction process is very slow and that an assumption of adiabatic conditions for the cavity is probably a good approximation. The heat balance, of course, tends to confirm this hypothesis.

Furthermore, and perhaps most important, the heat balance corroborates the hypotheses made concerning hydraulic events which occurred prior to day 100. The inflow to the cavity calculated in conformance with these hypotheses was used in determining ΔH_3, a major fraction of the total heat in the cavity. Large variations in the hydraulic properties of the system, the day of condensation, or the cavity radius would tend to offset the previously indicated agreement.

WATER QUALITY OF THE CANNIKIN-PERTURBED HYDROLOGIC SYSTEM

GENERAL DISCUSSION OF QUALITY OF THE WATER SAMPLES OBTAINED FROM UA–1–P1

All water samples from UA–1–P1 were obtained with a thief sampler — that is, the sampling device was lowered to the desired level in the hole, ports were opened to allow water to enter, ports closed, and the device raised to land surface. Use of this method provided water samples from the drill stem, presumed to be representative of water in the cavity/chimney region. Surging with nitrogen or air was done prior to some of the sampling to increase the probability that drill-stem samples would contain a large proportion of formation water. As we shall see, the method of hole completion played a dominant role in the analytical results from samples obtained through thief sampling of UA–1–P1.

RESULTS FROM EARLY SAMPLING, FEBRUARY AND JULY 1972

The first sample retrieved from the hole was on February 20, 1972 (day 106). The postulated condition of the chimney region at that time is indicated on plate 1*H* and the analytical results are in table 2. Between February 20, 1972, and April 10, 1972 (day 156), at least 12 700 gal (48 m³) of water of unknown composition, but probably from Constantine Spring, had been poured down the drill stem. From this date to July 15, 1972 (day 251), the hole remained undisturbed, water entering the perforations at zone A and raising the column of water which occupied the drill stem on day 156. The postulated conditions in the chimney region and the drill stem on day 251 are illustrated on plate 1*J*. Sources of samples taken from various points in the drill stem on days 252 through 255 are shown on plate 1*J* also. Since the bottom of the introduced-water column represented water residing opposite zone A on day 156, all water in the drill stem below this point represented water entering zone A on a later date, the exact date being determined by the rate of water-level rise as shown in figure 4. By comparing the sampling depths with the water-level data, approximate values were obtained for the dates each sample entered the drill stem at zone A, and, thus, these samples became an estimate of water quality in the cavity in the vicinity of zone A on those dates.

Because it was suspected that the addition of foreign water prior to day 156 might contaminate subsequent samples, the July sample results were examined for indications of dilution by Constantine Spring water (table

TABLE 2. — *Chemical and radiochemical analyses of samples from UA–1–P1 collected from February to July 1972*

[Values in parentheses are corrected for dilution by lithium-tagged water placed into UA–1–P1 prior to perforating activities at zones B through F in July 1972]

Sample identification				Dissolved chemical constituents		Dissolved radiochemical constituents			Suspended radiochemical constituents			Distribution coefficient for gross beta/gamma activity
Location name	Date of collection	Distance above arbitrary subsurface datum		Lithium	Total solids	Gross alpha as natural uranium	Gross beta/gamma as ^{137}cesium	Tritium	Suspended solids	Gross alpha as natural uranium	Gross beta/gamma as ^{137}cesium	
		ft	m	meq/L	mg/L	pCi/L	pCi/L	pCi/L	mg/L	pCi/g	pci/g	ml/g
	2–20–72	338	103	0.03	130	8.8	1.7×10^3	1.4×10^7	...	...	...	...
	7–16–72	3207	978	.02	1600	49	1.6×10^2	9.0×10^8	2100	<1.8	3.0×10^2	1.9×10^3
	7–17–72	2714	827	.01	1000	8.8	4.8×10^2	1.7×10^9	2300	<2.7	1.2×10^3	2.5×10^3
	7–17–72	2230	680	.01	120	1.3	2.9×10^3	2.4×10^9	700	<3.6	2.0×10^4	6.9×10^3
	7–17–72	1733	528	.03	380	15	8.6×10^1	1.8×10^7	3600	<1.3	1.1×10^2	1.3×10^3
	7–18–72	1196	365	.04	240	20	2.0×10^2	9.8×10^6	1600	<4.7	2.8×10^2	1.4×10^3
	7–18–72	1186	362	.03	220	8.5	1.7×10^2	4.9×10^6	1300	<4.3	4.4×10^2	2.6×10^3
	7–19–72	646	197	.02	230	6.9	2.9×10^2	8.7×10^7	1200	<3.6	1.2×10^3	4.1×10^3
Zone B	7–22–72	654	199	4.61	700 (700)	14 (23)	3.4×10^2 (5.5×10^2)	1.4×10^7 (2.3×10^7)	95	<6.3	6.2×10^3	1.8×10^4 (1.1×10^4)
Zone C	7–23–72	957	292	3.03	460 (380)	5.3 (7.1)	1.4×10^2 (1.8×10^2)	2.1×10^5 (2.8×10^5)	55	<7.3	1.5×10^4	1.1×10^5 (8.3×10^4)
Zone D	7–24–72	1255	383	2.31	2200 (2600)	67 (83)	4.6×10^2 (5.7×10^2)	1.3×10^7 (1.6×10^7)	350	<4.3	2.9×10^4	6.3×10^4 (5.1×10^4)
Zone E	7–25–72	1544	471	.81	230 (200)	18 (19)	1.2×10^2 (1.3×10^2)	5.4×10^1 (5.8×10^1)	76	<5.3	7.1×10^3	5.9×10^4 (5.5×10^4)
Zone F	7–26–72	1818	554	.53	2600 (2700)	98 (100)	4.1×10^2 (4.3×10^2)	8.9×10^6 (9.3×10^6)	360	5.8	4.9×10^4	1.2×10^5 (1.1×10^5)

3), the most probable source of the foreign water. Unfortunately, only lithium and dissolved solids values are available for comparison of the July samples with Constantine Spring. This is insufficient for a positive evaluation. However, the sample collected about 160 ft (49 m) below the bottom of the introduced-water column (pl. 1*J*) contains more than eight times the dissolved solids, has more than an order of magnitude greater lithium content than Constantine Spring, and has the highest dissolved-solids content of the suite of samples collected which indicates little contamination.

Although the July 1972 samples from UA–1–P1 identified in table 2 represent the earliest samples collected, they were in fact collected rather late in the chimney-filling process. (See pl. 1*H, I, J.*) During the period of chimney-filling history represented by these samples the major portion of the chimney is being filled, the cavity region contains water representative of a prior accumulation in the chimney which has drained into the cavity region following steam condensation. It is interesting that none of the samples approach formation water expected at the depth of zone A (aquifer 3B). (See table 3 for analyses of water from this aquifer.) Two of the samples have dissolved solids and lithium values which are similar to those of aquifers 1 and 2 (table 3), and one sample is lower in dissolved solids than any permanent body of surface water listed in table 3. This latter sample is believed to be composed of a large percentage of condensed steam from the cavity — note its high radioactivity. Why do these samples not have a composition more nearly that of the contributing aquifers? The following discussion is offered as explanation.

LOCALIZED FLOW NEAR THE UA–1–P1 DRILL HOLE

Figure 9 shows three temperature profiles in UA–1–P1 and their relation to hole construction. The predetonation natural thermal gradient, as measured in hole UA–1 after a long period of equilibration, is also shown for comparison. Profiles above the top of cement holding the 13^3/$_8$-in. (340-mm) casing are well below normal; in fact, they are very close to the mean annual surface temperature of Amchitka of 40°F (4°C) (Gonzalez and Wollitz, 1972), indicating the source of flow during the annulus between the drilled hole and casing is of shallow origin. Between the top of the upper and the bottom of the lower cemented intervals flow is restricted sufficiently to allow the temperature to approach normal; below the bottom of the 9^5/$_8$-in. (240-mm) casing significant flow resumes, and the temperature is subnormal until the cavity region is reached. Here, the curves begin to differ significantly from each other. The April 9 log is lower in temperature than one made 101 days later (July 20). This is believed to be caused by the introduced water discussed above. The log of July 20, made prior to perforating intervals B through F, is taken as representative of average cavity temperatures. The slight gradient reversals are probably caused by regions of higher than average fracture

TABLE 3. — *Chemical and radiochemical analyses of samples collected at selected locations on Amchitka Island, Alaska*

Sample identification			Dissolved chemical constituents									Dissolved radiochemical constituents	
Location name	Depth below land surface of collection point		Silica, (SiO_2)	Magnesium (Mg^{+2})	Calcium (Ca^{+2})	Lithium (Li^{+1})	Sodium (Na^{+1})	Potassium (K^{+1})	Sulfate (SO_4^{-2})	Chloride (Cl^{-1})	Total solids	Gross alpha as natural uranium	Gross beta/ gamma as ^{137}cesium
	ft	m	mg/L	meq/L	meq/L	meq/L	meq/L	meq/L	meq/L	meq/L	mg/L	pCi/L	pCi/L
Constantine Spring[1]	...	...	15	0.13	0.05	<0.001	2.4	0.12	0.08	1.1	180	<3	5.0
White Alice Creek[2]	...	...	17	.17	.19	<.001	1.4	.05	.06	1.3	150	<0.5	7.7
Cannikin Lake	...	...	19	.18	.25	<.001	2.9	.10	.47	2.0	250	1.9	4.7
Precipitation at south hanger[3]	...	...	...	.06	.06	...	.35	.01	.10	.29	e40	...	...
Lake 100 meters west of milepost 12	...	...	2.6	.10	.06	...	.85	.02	.06	.82	70	...	...
Lake 980 meters ESE. of Cannikin ground zero	...	...	...	.31	.32	<.001	3.0	.03	.46	1.8	e250	...	...
Seep 3	...	...	25	.03	.06	...	3.8	.02	.12	2.4	250	1.0	5.6
Well HTH-1	602-770	183-235	11	.02	.10	.001	6.1	.02	.87	1.8	310	3.0	4.2
Well HTH-1	746-914	227-279	12	.07	.70	<.001	7.4	.02	2.9	1.7	570	2.2	4.6
Well HTH-3	169	52	17	.08	.17	<.001	4.6	.07	.33	1.9	330	3.1	1.5
Well UA-1, aquifer 3B	5910	1801	28	<.01	5.5	.01	48	.21	2.9	54	e4600	...	...
Well UAE-1, aquifer 1	1600-1850	488-564	13	.04	3.0	.01	18	.15	1.2	17	1500	...	...
Well UAE-1, aquifer 2	2490-2580	759-786	28	.10	2.6	.10	13	.13	3.1	15	1500	...	...
Well UAE-1, aquifer 3B	5650-5850	1722-1783	22	.01	7.2	<.01	52	.20	3.4	58	4300	<3.3	<5.0
Well UAE-1, aquifer 3B	5000-7000	1524-2134	18	<.01	7.7	.01	41	.26	2.9	49	4600	<15	18

[1]Average of 17 samples collected from October 1964 to July 1972.
[2]Average of 9 samples collected from August 1967 to April 1972.
[3]Average of 4 samples.
e, Estimated from specific-conductance data.

conductivity. The log of July 27 shows the effect of perforating the five intervals above zone A. The local hydraulic conditions in the vicinity of the drill stem affected the composition of subsequent samples. We shall see just how in the discussion of samples obtained during perforating operations and during later sampling episodes.

INTERPRETATION OF VERTICAL DISTRIBUTION OF WATER QUALITY IN THE CANNIKIN CAVITY

Samples from intervals B through F (table 2) were first obtained immediately after sequential perforating and surging. The sequence of perforating was from the lowest interval (B) to the highest (F). Since the hydraulic potential decreased slightly with depth, it was slightly higher in each zone perforated than in those perforated previously; therefore, water sampled after perforating should have been that which had just entered the drill stem.

In order to assess the effectiveness of surging in inducing water from outside to enter the drill stem, fresh water to which lithium chloride had been added as a tracer was introduced into the drill stem in an amount slightly more than necessary to displace the water already present. This tracer was added just prior to perforating zones B through F. The data in table 2 associated with the designated zones B through F are the results of sampling after perforating each zone and surging. The sample from zone B was the most contaminated (contained 38 percent tracer water), and the sample from zone F, the least (contained 4 percent tracer water). All the raw data were corrected when possible for tracer-water contamination; these corrected results are included in parentheses in the tables. The samples from zones D and F are high in dissolved solids and in radioactivity, but are from zones showing low gamma activities on the gamma log. (See fig. 10 for the results obtained from gamma-logging and their relation to the perforated intervals, zones B through F.) The samples from zones C and E are very low in dissolved solids and contain considerably less radioactivity but are from zones which logged high in gamma activity. The sample from zone B is both high in radioactivity and from a zone of high gamma activity. Keeping in mind that the drill hole changed the local hydrologic conditions, it is reasonable to postulate that the zones of highest gamma activity are the zones of greatest hydraulic conductivity (note slight temperature reversals at zones B and C on the temperature log), having carried considerable radioactive water during infill and, since drilling of the reentry hole, carried major amounts of near-surface-source water flowing along the route penetrated by the hole. The result is that radionuclides have been deposited on the surfaces of these hydraulically conductive routes during the infill

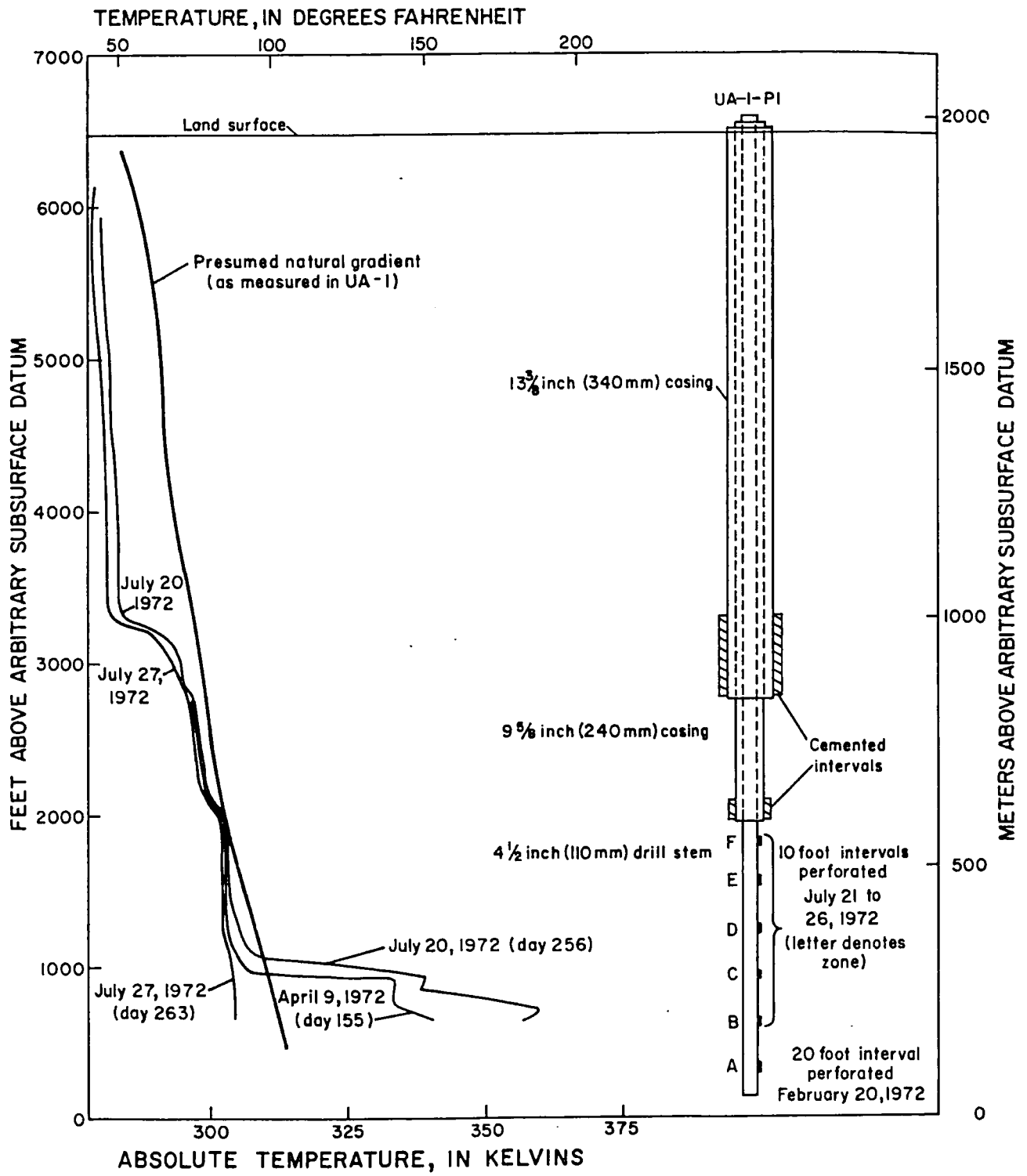

FIGURE 9. — Temperature profiles in UA–1–P1 and their relationship to hole construction and natural gradient.

process; the carrier solutions have subsequently been flushed by the water flowing near the reentry hole, which has resulted in fresh water of low radioactivity in zones of high gamma activity. Conversely, the zones exhibiting low gamma activity still contain water of approximate cavity-infill water dissolved solids and radioactivity but have not accumulated gamma activity over and above that of infill water composition, owing to relatively restricted flow conditions. Radioactivity is anticipated to increase with depth in the cavity region because of leaching by downward percolating of infill water; therefore, it is not surprising that the lowest

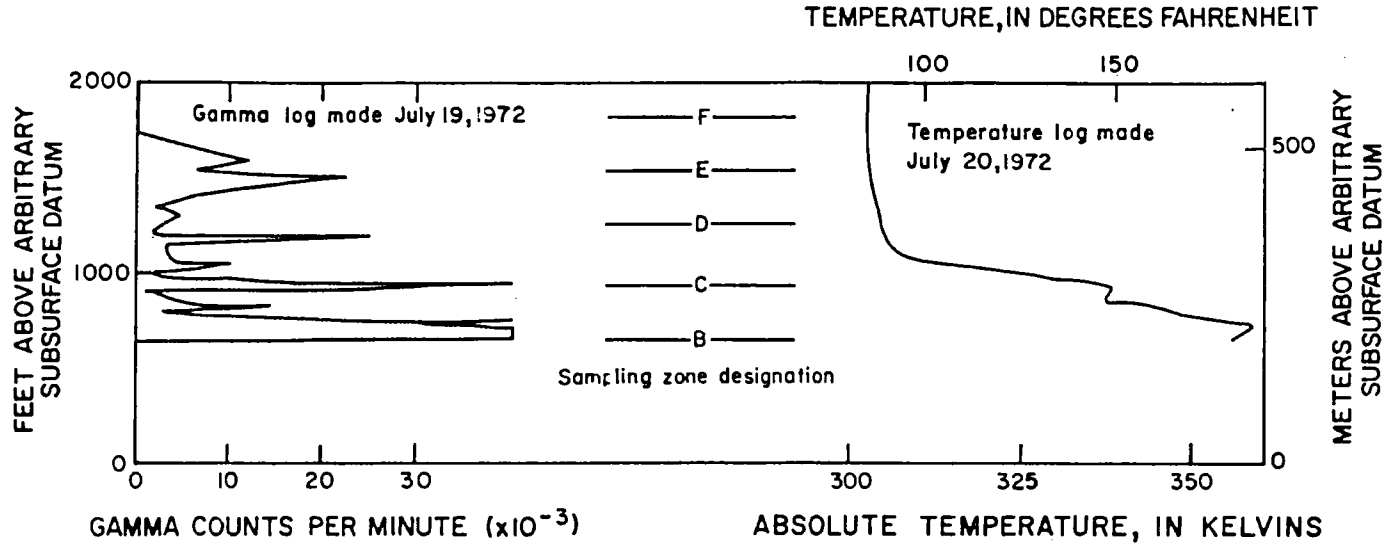

FIGURE 10. — Temperature- and gamma-log profiles in UA–1–P1 and their relation to sampling zones B through F.

zone (B) shows sufficient radioactivity to overshadow the above effects.

Three additional visits to the UA–1–P1 site were made and samples thiefed from the drill stem both before and after surging. These will first be discussed separately.

RESULTS FROM THE OCTOBER 1972 SAMPLING

The samples obtained from points above zone B prior to surging (October 13–15, 1972) are generally more saline than those obtained after surging (October 18–19, 1972). The data are shown in table 4. The temperature log made prior to sampling (identical to the July 27, 1972, log in fig. 9) indicated downward flow in the vicinity of the drill stem. However, the analytical results show little or no flow in the drill stem above zone B, suggesting that the downward flow was outside of the drill stem and that the perforations in zones C through F were plugged. The analytical results of post-surging samples confirm this hypothesis as nearly all samples decrease in dissolved- and radioactive-constituent concentration. Zone D is the exception, and will be discussed later. (See below.)

RESULTS FROM THE JANUARY 1973 SAMPLING

The analytical results from samples collected during January 1973 are found in table 5. Once again, the samples obtained before surging (January 17–18, 1973) are different from those obtained after surging (January 21–22, 1973), but the differences are less pronounced. The post-surging results from zone D display behavior similar to that of the October 1972 sampling — that is, a less pronounced decrease in dissolved solids and radioactivity than observed at other zones. Zone D probably is producing water from a region outside the drill hole in conjunction with fresher water flowing down the drill hole from above. This fresher water enters zones E and F, flows down the drill stem and mixes with the more saline (and more radioactive) water entering at zone D. The same fresh water entering zones E and F is apparently available for entry at zones B and C. A FLO-PAK[1] log (essentially a flowmeter survey to determine quantity of water flowing vertically in a hole) produced the data shown in figure 11. These results, obtained after surging, show only a small contribution to

[1] The use of any brand name in this report is for identification purposes only and does not imply endorsement by the U.S. Geological Survey.

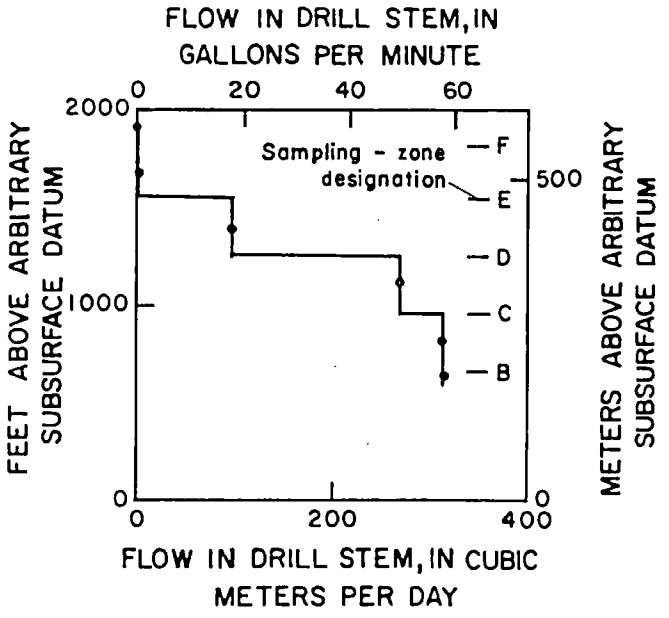

FIGURE 11. — Results of FLO-PAK survey in UA–1–P1.

TABLE 4. — *Chemical and radiochemical analyses of samples from UA–1–P1, collected October 1972*

[Values in parentheses are corrected for dilution by lithium-tagged water placed into UA–1–P1 prior to perforating activities at zones B through F in July 1972. Leaders (. . .) indicate no data]

Sample identification				Dissolved chemical constituents								Dissolved radiochemical constituents			Suspended radiochemical constituents			Distribution coefficient for gross beta/gamma activity
Location name	Date of collection	Distance above arbitrary subsurface datum		Magnesium (Mg^{+2})	Calcium (Ca^{+2})	Lithium (Li^{+1})	Sodium (Na^{+1})	Potassium (K^{+1})	Chloride (Cl^{-1})	Sulfate (SO_4^{-2})	Total solids	Gross alpha as natural uranium	Gross beta/gamma as ^{137}cesium	Tritium	Suspended solids	Gross alpha as natural uranium	Gross beta/gamma as ^{137}cesium	
		ft	m	meq/L	meq/L	meq/L	meq/L	meq/L	meq/L	meq/L	mg/L	pCi/L	pCi/L	pCi/L	mg/L	pCi/g	pCi/g	ml/g
(1)	10–13–72	6082	1854	...	...	0.08	...	...	...	...	1200	9.1	1.1×10^2	8.4×10^3	400	4.2	3.5×10^2	3.2×10^3
(1)	10–13–72	3662	1116	...	...	1.3	...	...	...	...	620 (610)	<2.2	8.7×10^1 (9.7×10^1)	3.3×10^4 (3.7×10^4)	260	6.5	8.1×10^2	9.3×10^3 (8.4×10^3)
(1)	10–13–72	1833	559	0.05	6.2	3.3	24	0.13	27	2.1	3200 (4100)	<8.5	2.1×10^2 (2.9×10^2)	3.3×10^7 (4.5×10^7)	2,200	5.0	4.1×10^2	2.0×10^4 (1.4×10^4)
(1)	10–13–72	1695	517	.03	9.2	.45	42	.12	51	2.8	4200 (4300)	<11	1.6×10^2 (1.7×10^2)	5.0×10^7 (5.2×10^7)	430	<4.4	4.0×10^3	2.5×10^4 (2.4×10^4)
Zone E	10–13–72	1549	472	.03	8.0	.27	36	.13	45	2.3	3800 (3900)	<18	1.3×10^2	4.3×10^7 (4.4×10^7)	320	<6.2	4.7×10^3	3.6×10^4
(1)	10–14–72	1405	428	...	7.5	.20	29	...	45	...	3600	<13	1.5×10^2	3.8×10^7 (3.9×10^7)	550	5.6	3.6×10^3	2.4×10^4
Zone D	10–14–72	1260	384	.03	7.0	.17	26	.13	39	4.1	3300	<12	1.6×10^2	3.5×10^7 (3.6×10^7)	440	<5.0	4.1×10^3	2.6×10^4
(1)	10–14–72	1112	339	...	3.2	.68	17	...	21	...	1700	<4.4	1.9×10^2 (2.0×10^2)	3.2×10^7 (3.4×10^7)	540	6.7	3.7×10^3	1.9×10^4 (1.8×10^4)
Zone C	10–14–72	962	293	.03	2.4	.59	12	.15	17	.79	1300	<5.5	1.8×10^2 (1.9×10^2)	2.6×10^7 (2.7×10^7)	430	7.2	3.0×10^3	1.7×10^4
(1)	10–14–72	813	248	...	4.0	.46	23	...	27	...	2000	<7.8	2.4×10^2 (2.5×10^2)	4.3×10^7 (4.4×10^7)	440	<5.4	3.9×10^3	1.6×10^4
Zone B	10–14–72	659	201	.02	.13	.08	4.4	.15	2.3	.12	340	<1.2	1.0×10^2	4.0×10^5	260	<6.5	1.6×10^3	1.6×10^4
(1)	10–15–72	642	196	.02	.13	.04	3.3	.15	1.7	.10	320	< .9	3.7×10^1	1.4×10^5	170	<8.2	1.7×10^3	4.6×10^4
Zone F	10–18–72	1818	554	.02	.10	.06	4.4	.15	2.1	.12	350	< .9	4.2×10^1	4.3×10^4	220	7.3	1.4×10^3	3.3×10^4
Zone E	10–18–72	1544	471	.02	.14	.04	3.5	.15	1.9	.11	330	<1.2	5.4×10^1	7.4×10^4	240	7.9	1.4×10^3	2.6×10^4
Zone D	10–18–72	1255	383	.03	.42	.50	13	.16	11	.66	1200	<4.1	1.3×10^2 (1.4×10^2)	6.1×10^6 (6.4×10^6)	770	<4.3	2.1×10^3	1.6×10^4 (1.5×10^4)
(1)	10–18–72	1112	339	...	.10	.02	4.8	...	1.9	...	360	<1.3	4.2×10^1	1.1×10^5	160	<6.9	1.1×10^3	2.6×10^4
Zone C	10–19–72	957	292	.02	.08	.04	4.4	.14	1.9	.11	340	<1.3	4.0×10^1	1.0×10^5	220	7.3	1.3×10^3	3.2×10^4
(1)	10–19–72	813	248	.02	.09	.02	5.2	.15	2.0	.11	380	<1.1	3.4×10^1	1.3×10^5	200	<7.5	1.1×10^3	3.2×10^4
Zone B	10–19–72	654	199	.02	.07	.03	4.2	.14	2.0	.11	340	<1.2	3.6×10^1	1.4×10^5	200	<6.0	1.4×10^3	3.9×10^4
(1)	10–19–72	643	196	...	.08	.02	4.3	...	2.1	...	410	1.9	5.0×10^1	1.3×10^5	140	<7.1	1.5×10^3	3.0×10^4

[1] No designation.

TABLE 5. — *Chemical and radiochemical analyses of samples from UA–1–P1 collected January 1973*

[Values in parentheses are corrected for dilution by lithium-tagged water placed into UA–1–P1 prior to perforating activities at zones B through F in July 1972]

Sample identification				Dissolved chemical constituents								Dissolved radiochemical constituents			Suspended radiochemical constituents			Distribution coefficient for gross beta/gamma activity
Location name	Date of collection	Distance above arbitrary subsurface datum		Magnesium (Mg^{+2})	Calcium (Ca^{+2})	Lithium (Li^{+1})	Sodium (Na^{+1})	Potassium (K^{+1})	Chloride (Cl^{-1})	Sulfate (SO_4^{-2})	Total solids	Gross alpha as natural uranium	Gross beta/gamma as ^{137}cesium	Tritium	Suspended solids	Gross alpha as natural uranium	Gross beta/gamma as ^{137}cesium	
		ft	m	meq/L	meq/L	meq/L	meq/L	meq/L	meq/L	meq/L	mg/L	pCi/L	pCi/L	pCi/L	mg/L	pCi/g	pCi/g	ml/g
(1)	1–17–73	5982	1823	0.02	0.07	0.03	7.4	0.15	2.2	0.45	600	<1.7	3.1×10^1	1.1×10^4	240	<5.4	9.6×10^2	3.1×10^4
Zone F	1–17–73	1818	554	.04	5.2	.43	27	.13	34	1.8	2700	<9.5	8.9×10^1	3.2×10^7	780	<3.6	2.4×10^3	2.7×10^4
											2800		(9.2×10^1)	(3.3×10^7)				(2.6×10^4)
Zone E	1–17–73	1544	471	.05	.13	.72	13	.15	4.2	6.2	690	<1.9	3.7×10^1	1.0×10^5	600	<4.7	1.7×10^3	4.6×10^4
													(3.9×10^1)	(1.1×10^5)				(4.4×10^4)
Zone D	1–18–73	1255	383	.03	6.5	.16	33	.13	39	1.7	2900	<10	8.8×10^1	3.7×10^7	440	<5.0	2.3×10^3	2.6×10^4
													(8.9×10^1)					
Zone C	1–18–73	957	292	.06	.19	.03	11	.15	3.4	.75	830	4.0	2.7×10^1	2.0×10^5	250	<5.2	3.0×10^2	1.1×10^4
Zone B	1–18–73	654	199	.05	.15	.03	10	.15	3.1	.66	780	<2.2	2.5×10^1	1.4×10^5	210	<4.3	4.8×10^2	1.9×10^4
(1)	1–18–73	644	196	.05	.13	.03	9.1	.14	3.4	.56	620	3.0	1.9×10^1	1.4×10^5	210	<5.7	6.7×10^2	3.5×10^4
Zone F	1–21–73	1818	554	.07	.21	.02	12	.14	3.7	.93	940	4.4	2.7×10^1	6.8×10^4	210	<5.7	4.8×10^2	1.8×10^4
Zone E	1–21–73	1544	471	.07	.23	.02	13	.14	4.0	1.0	970	3.7	3.5×10^1	4.6×10^4	220	5.9	5.0×10^2	1.4×10^4
Zone D	1–21–73	1255	383	.04	4.0	.04	26	.13	28	1.2	2100	<7.8	6.6×10^1	2.6×10^7	590	<4.8	1.5×10^3	2.3×10^4
Zone C	1–21–73	957	292	.06	.22	.02	11	.14	3.7	.85	830	<3.2	2.6×10^1	1.4×10^5	160	<5.0	6.1×10^2	2.3×10^4
Zone B	1–22–73	654	199	.06	.27	.02	13	.13	4.0	1.0	990	<4.8	2.9×10^1	1.5×10^5	170	<4.7	8.2×10^2	2.8×10^4
(1)	1–22–73	644	196	.07	.25	.02	12	.14	4.0	.95	930	<4.4	2.6×10^1	1.7×10^5	220	<5.9	4.5×10^2	1.7×10^4

[1] No designation.

vertical flow in the drill stem from zone F (less than 1 percent), about 31 percent of the total flow is contributed by zone E, 55 percent by zone D, and an additional 14 percent by zone C. Zone B does not seem to contribute, and may actually be an exit point for, some of the water flowing down the drill stem.

The perforations in the drill stem apparently became plugged between October 1972 and January 1973, but perhaps not as severely as before the October 1972 sampling.

RESULTS FROM THE MAY 1973 SAMPLING

The differences between presurging (May 2–4, 1973) and postsurging (May 8–9, 1973) samples, reported in table 6, are again evident, but to a lesser degree than in any of the previous sampling episodes. The downhole flow pattern is evident, as before, from temperature and FLO-PAK logs (not illustrated but virtually identical to the July 27, 1972, temperature log illustrated in figure 9 and the FLO-PAK log in figure 11) and zone D still contributes the most saline and radioactive water.

Figure 12 shows the relationship between dissolved solids and tritium concentration for samples obtained from zones B through F during the July 1972, October 1972, January 1973, and May 1973 samplings. Although there is considerable scatter in the data, two relationships are evident — (1) samples with higher dissolved-solids values generally have higher tritium radioactivities, and (2) the range of dissolved-solids values (and, therefore, radioactivities) decreases from October 1972 to May 1973. This is consistent with the hypothesis that the cavity region was initially filled mainly by formation water from aquifers 3B, 3A, 2, and 1, which have dissolved-solids values in the range 1500 to 4500 mg/L. This water, which would be expected to contain the major amount of radioactivity (ignoring the problems associated with condensed steam estimated to account for about 3 percent of total cavity water), is being diluted by near-surface water which is being recharged to the cavity region by way of the UA–1–P1 drill hole. As this process continues, some mixing of the native and recharged waters is expected and confirmed by the decreasing range in dissolved-solids and radioactivity values from October 1972 to May 1973. A second phenomenon is occurring concurrently with mixing: the reaction of freshly recharged water with the subsurface aquifer matrix. A more detailed discussion of these processes follows the description of the natural water quality in the vicinity of the Cannikin site (See p. D19, D21.)

WATER QUALITY AS A DESCRIPTOR OF THE FLOW SYSTEM

To better explain changes observed in the samples from UA–1–P1, an attempt was made to define the chemical changes accompanying evolution of groundwater composition in the vicinity of the Cannikin site, in the belief that an understanding of the natural system would lead to an understanding of the perturbed system.

From published data (Beetem and others, 1971; Schroder and Ballance, 1973) and unpublished data in U.S. Geological Survey files at Denver, Colo., it was determined that waters from surface, shallow subsurface, and deep subsurface systems could be distinguished from each other most easily by their respective total dissolved-solids content and sodium ion to chloride ion ratios (Na/Cl). Results of plotting data obtained from those systems and from the Cannikin chimney and cavity during the several sampling episodes are shown in figure 13. Analytical data for samples from these sites used in constructing figure 13 are presented in tables 3 through 6.

Water recharged to shallow aquifers on Amchitka begins as precipitation; the composition of precipitation on the island is affected by local conditions, mainly sea spray. Thus, the composition varies considerably from time to time, depending on local weather conditions, with high-dissolved-solids precipitation exhibiting Na/Cl ratios resembling that of sea water. The value plotted in figure 13 is an average of the Na/Cl ratio of four samples that were low in dissolved-solids content and are believed to represent average precipitation. When precipitation becomes part of the surface-water system, it reacts with the various organic and inorganic components at and near ground surface. The major result is the increase in sodium ion concentration relative to chloride ion as the concentration of dissolved solids increases. The large scatter in data among the surface-water locations plotted reflects the wide variety of surface-water environments present on Amchitka. A very small fraction of the surface water probably enters the shallow ground-water system (arbitrarily defined as less than about 1000 ft or 305 m in depth), but that which does continues to react with the volcanic-rock matrix of the hydrologic system, increasing the Na/Cl ratio further.

The natural vertical hydraulic conductivity between the shallow aquifers (represented by wells HTH–1 and HTH–3) and the deeper aquifers (represented by aquifers 1, 2, and 3B in wells UAE–1 and UA–1) is apparently very low, resulting in the large diffusion zone in the Ghyben-Herzberg lens proposed for Amchitka by Fenske (1972). The location in figure 13 of plots of samples from these deeper aquifers suggest that these aquifers are within a very large zone of diffusion (or mixing) between a hypothetical sea water of present-day composition and shallow ground water of undetermined composition but probably similar to waters of wells HTH–1 and HTH–3.

Examination of plotted data for samples obtained from UA–1–P1 during the three major sampling

TABLE 6. — *Chemical and radiochemical analyses of samples from UA–1–P1 collected May 1973*

[Values in parentheses are corrected for dilution by lithium-tagged water placed into UA–1–P1 prior to perforating activities at zones B through F in July 1972]

Sample identification				Dissolved chemical constituents						Dissolved radiochemical constituents			Suspended radiochemical constituents			Distribution coefficient for gross beta/gamma activity
Location name	Date of collection	Distance above arbitrary subsurface datum		Calcium (Ca^{+2})	Lithium (Li^{+1})	Sodium (Na^{+1})	Chloride (Cl^{-1})	Sulfate (SO_4^{-2})	Total solids	Gross alpha as natural uranium	Gross beta/gamma as ^{137}cesium	Tritium	Suspended solids	Gross alpha as natural uranium	Gross beta/gamma as ^{137}cesium	
		ft	m	meq/L	meq/L	meq/L	meq/L	meq/L	mg/L	pCi/L	pCi/L	pCi/L	mg/L	pCi/g	pCi/g	ml/g
(1)	5–2–73	5982	1823	0.13	0.04	7.8	2.7	0.20	620	16	1.5×10^1	1.9×10^4	150	42	3.3×10^2	2.2×10^4
(1)	5–2–73	2781	848	.07	.30	8.7	3.1	.18	670	<9.3	2.1×10^1 (2.2×10^1)	2.4×10^4 (2.5×10^4)	540	<14	2.8×10^2	1.3×10^4
(1)	5–2–73	2003	611	.07	.39	8.7	3.1	.17	670	<9.3	2.3×10^1 (2.4×10^1)	2.5×10^4 (2.6×10^4)	460	37	4.8×10^2	2.1×10^4 (2.0×10^4)
Zone F	5–3–73	1818	554	.23	.04	10	2.6	.71	820	16	1.9×10^1	8.7×10^4	100	42	7.2×10^2	3.8×10^4
(1)	5–3–73	1695	517	.40	.16	14	10	.44	1000	<14	2.5×10^1	8.7×10^5 (8.8×10^5)	560	<12	2.9×10^2	1.2×10^4
Zone E	5–3–73	1544	471	.27	.02	10	4.5	.67	850	<14	1.8×10^1	2.1×10^5	220	30	3.5×10^2	1.9×10^4
(1)	5–3–73	1405	428	.20	.03	9.1	2.8	.60	830	26	1.7×10^1	5.9×10^4	320	<18	8.8×10^1	5.2×10^3
Zone D	5–3–73	1255	383	.21	.01	9.1	2.8	.69	680	<9.3	1.4×10^1	3.7×10^4	300	<18	1.0×10^2	7.1×10^3
(1)	5–4–73	1112	339	.18	.01	7.8	2.6	.46	610	10	1.4×10^1	1.1×10^5	66	48	3.3×10^2	2.4×10^4
Zone C	5–4–73	957	292	.24	.01	7.8	2.6	.48	620	<8.9	1.2×10^1	1.3×10^5	73	33	3.8×10^2	3.2×10^4
(1)	5–4–73	813	248	.08	.09	7.0	2.4	.16	480	7.9	1.6×10^1	8.4×10^4	580	21	4.3×10^2	2.7×10^4
Zone B	5–4–73	654	199	.18	.01	7.4	2.5	.50	550	<7.8	1.3×10^1	1.2×10^5	100	<23	5.8×10^2	4.5×10^4
(1)	5–9–73	2003	611	.37	.01	4.8	2.0	.22	400	<6.7	8.4	1.5×10^4	130	23	1.9×10^2	2.3×10^4
Zone F	5–8–73	1818	554	.13	.03	6.1	2.1	.22	470	<8.0	1.0×10^1	3.7×10^4	83	<30	3.9×10^2	3.9×10^4
Zone E	5–8–73	1544	471	.16	.02	6.1	2.1	.23	490	8.3	1.0×10^1	4.7×10^4	91	<29	4.3×10^2	4.3×10^4
Zone D	5–9–73	1255	383	.17	.01	5.6	2.2	.22	510	11	1.1×10^1	8.4×10^4	130	38	5.7×10^2	5.2×10^4
Zone C	5–9–73	957	292	.16	.05	5.2	2.2	.22	510	<7.1	1.1×10^1	1.4×10^5	190	<16	1.5×10^2	1.4×10^4
Zone B	5–9–73	654	199	.12	<.01	6.1	2.2	.21	...	<4.5	8.7	1.0×10^5	240	<24	4.6×10^2	5.3×10^4

[1] No designation.

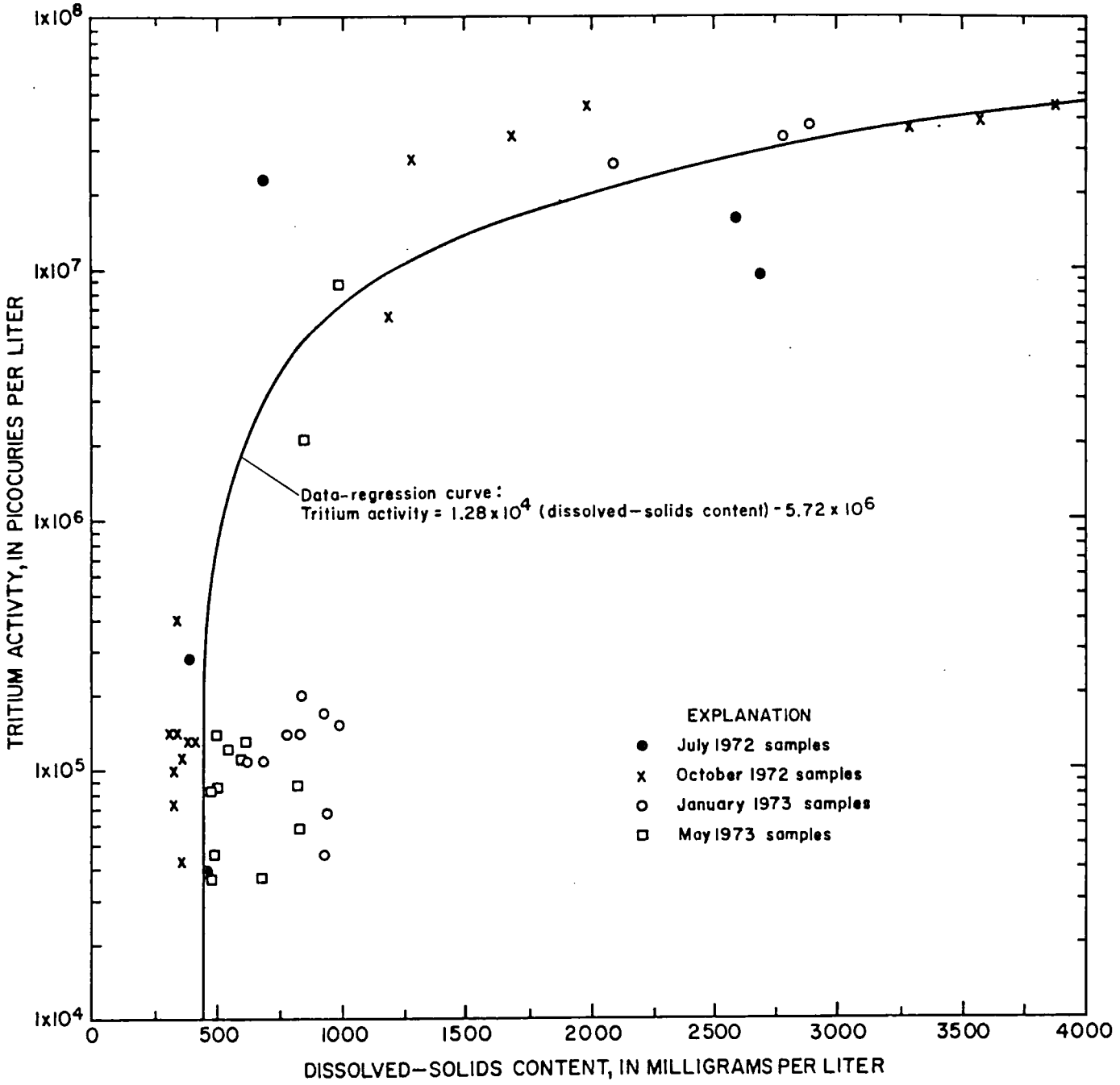

FIGURE 12. — Relationship between dissolved-solids content and tritium activity in selected samples from UA–1–P1.

episodes of October 1972 and January and May 1973 reveals the effect on water quality of fresh water being rapidly introduced into the subsurface system ("short-circuiting" the natural, unperturbed system). It was anticipated that this introduced water would undergo two phenomena: mixing with water from aquifers 1, 2, and 3 already present in the cavity, and reaction with the aquifer matrix on its path from near the surface downward to the cavity region. The data generally confirm the mixing and reaction hypothesis. The bulk of the data lying close to the postulated shallow-system reaction coordinate represents a combined subsurface reaction coordinate, paralleling the shallow-system coordinate, combined with mixing of water in various stages of reaction with native waters (for example, from aquifers 1, 2, and 3) residing in the cavity region. The reason for the five samples with Na/Cl ratios below those of aquifers 1 through 3 is not certain; possibly, reactive components in the cavity region produced by the nuclear explosion have introduced additional chloride or removed sodium, altering the predetonation water quality somewhat.

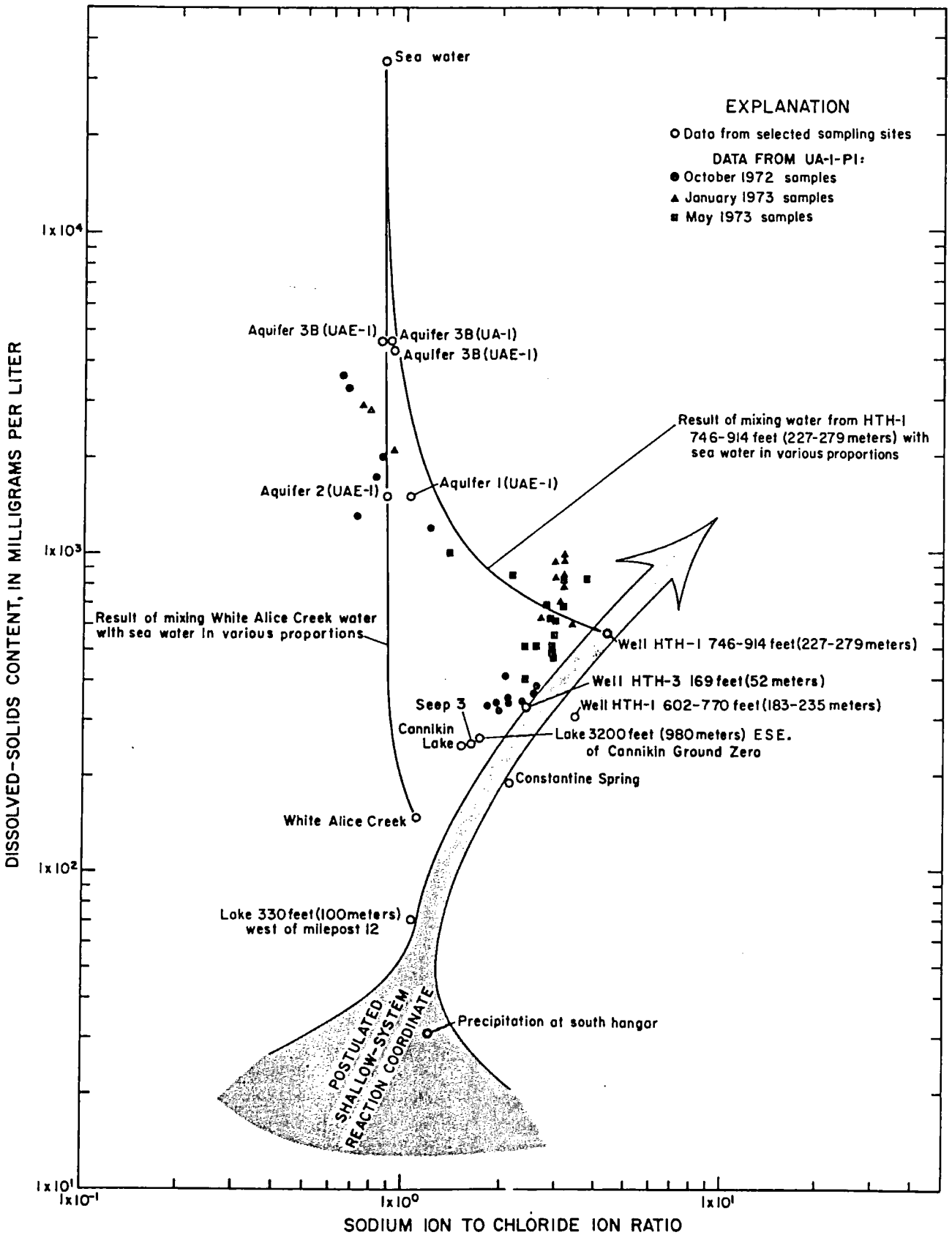

FIGURE 13.. — Chemical evolution of surface water and shallow ground water and its relation to water from UA–1–P1 and other subsurface water.

RADIOACTIVITY IN CAVITY WATER

As previously indicated, study of the tables containing radiochemical data from UA–1–P1 reveals the general increase in radioactivity with increased dissolved-solids content of the samples. Because of its 12-year half-life, the tritium content seems to correlate better than gross beta/gamma activity with dissolved-solids content (the average beta/gamma activity half-life was determined and will be discussed later). This correlation supports the hypothesis that the major infill to the cavity and chimney was from aquifers 1, 2, and 3 and that, by the time the perturbation in the flow system caused by the drilling of UA–1–P1 occurred, at least some of the radioactivity produced by the explosion had been distributed throughout the more saline subsurface water from aquifers 1, 2, and 3 in the cavity region. A few exceptions to this generalization exist in data obtained during July 16–19, 1972, as reported in table 2. The samples representing water that entered zone A during the period of days 160–236 are generally higher in radioactivity for a given dissolved-solids content than those samples obtained later, and representing later times in the cavity history. Some of the samples undoubtedly contain condensed steam from the cavity, which is expected to harbor large amounts of tritium and radionuclides with gaseous precursors — for example, note that the sample collected at 2230 ft (680 m) on July 17, 1972, has the lowest dissolved solids but the highest tritium and gross beta/gamma activities. Once the effect of condensed steam has been minimized by convective mixing stimulated by the inception of significant downward flow at the sampling points (that is, after July 20, 1972), the relationship between dissolved solids and radioactivity is simplified, representing combinations of nonradioactive fresh water with radioactive water of a salinity roughly comparable to bulk infill to the cavity and chimney. It was anticipated that a plot of salinity (as dissolved solids) versus radioactivity, extrapolated to a salinity value similar to that of aquifer 3B, would result in a reasonable estimate of bulk cavity-water radioactivity (that is, hydrologic-contaminant source term), but the scatter of the data was too great for a reliable extrapolation. It is indeed unfortunate that samples could not be obtained by pumping, which would have thereby minimized the effect of the fresh water introduced through the UA–1–P1 drill hole.

BETA/GAMMA ACTIVITY AS AN INDICATOR OF RADIONUCLIDE-SORPTION DISEQUILIBRIUM

Although the samples collected from the reentry hole probably were not representative of bulk cavity water, the radioactivity present in the samples was reasoned to be a representative sample of isotopes present in the aqueous phase but at lower concentration. Thus, measurements of radioactivity in any given sample would be an indication of the characteristics possessed by the true radioactive source water. Because very little alpha activity was observed in any of the samples and specific radionuclide analysis was prohibited by cost and manpower limitations, the changes with time in the gross beta/gamma activity (except for tritium) were chosen to describe changes in aqueous-phase radioactivity. Recounting of planchets prepared for gross beta/gamma analysis and calibrated using cesium-137 yielded changes in radioactive content with time for a given sample; all such recounts made on samples collected during a given sampling episode (for example, October 1972) from locations at or below zone F together with the initial counting data and the time in days which elapsed between the first counting and the recount were substituted into equation 1 to determine the average half-life for beta/gamma activity for each sample during that period.

$$t_{1/2} = \frac{-0.693t}{\ln(A/A_0)},$$

where

$t_{1/2}$ is the average half-life, in days, of the beta/-gamma activity for the time period of interest;

t is the length, in days, of the time period of interest; A_0 is the concentration of radioactivity at the beginning of the time period;

A is the concentration of radioactivity at the end of the time period.

Some samples were recounted more than once and others (May 1973) unfortunately were not recounted at all. Arithmetic averages were computed of all half-lives determined on samples from a given sampling episode and plotted versus the day since zero time representing the midpoint of the first count to second count (or second count to third count) time period. Curve *A* of figure 14 resulted from these computations.

A different method of analysis was also undertaken. Figure 15 shows the gross beta/gamma data resulting from analysis of all samples obtained from below zone F in UA–1–P1 during the four major sampling episodes plotted against the dissolved-solids content. Regression lines were fitted to the data, and the intersection of those lines with the arbitrarily chosen dissolved-solids value of 1450 mg/L was determined. Inasmuch as it was assumed that the samples represented mixtures of radioactive water of specified dissolved-solids content with nonradioactive water of also specified, but lower, dissolved-solids content, differences in radioactivity between samples of given dissolved-solids content collected on two different dates should have represented

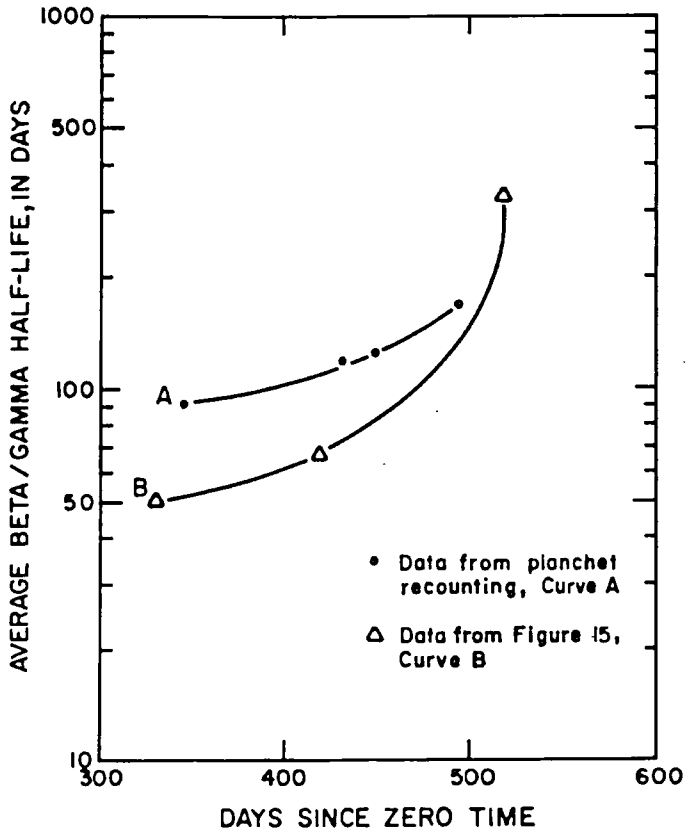

FIGURE 14. — Comparison of changes with time in the average beta/gamma activity determined by two methods — planchet recounting and data-regression analysis.

only radioactive decay. The average half-life of beta/gamma activity for the three intervals indicated in figure 15 was computed by using equation 1.

As shorter half-life activities decay to lower concentrations, the average half-life of remaining activity increases, as indicated by the values of $t_{1/2}$ shown in figure 15. These values were plotted versus the average counting day and resulted in curve *B* in figure 14. The plots of half-life versus time for the two methods used differ significantly through about day 480, the half-lives calculated using differences between two linear regressions being shorter. At first glance (refer again to fig. 14), the disagreement might be the result of the large scatter of data for July and October 1972 around their respective regression lines. This cannot be the cause, however, because similar scatter is present in computation of arithmetic means from planchet recounting data. The cause seems to lie in the assumption that only radioactive decay accounts for the decrease in activity in samples of given dissolved-solids content between two sampling episodes. Recall that the determination of half-life by the method of linear regression involves using the ratio of gross beta/gamma activities of two successive sampling episodes. If the value of *A* (eq 1) is lower than that which would result from radioactive decay alone, a smaller value of $t_{1/2}$ is computed. Therefore, the most probable reason for curve *B* of figure 14 lying below curve *A* is that a certain fraction of activity is being progressively removed from solution by sorption on particulate matter in the cavity region. Consequently, one would expect the distribution coefficient (K_d) to increase with time; this is not observed because the K_d values are very large (greater than 10 000 as found in tables 2, 4, 5, and 6) and small changes in solution concentration, which greatly affect the $t_{1/2}$ determinations, have little effect on K_d. Furthermore, as the bulk carrier solution becomes more dilute, radioactivity is expected to be transferred from the solution to the solid phase (that is, the sorption selectivity increases) and the calculated distribution coefficients should be negatively correlated to solution dissolved-solids content. This behavior was also not observed, the average distribution coefficient, $\sim 2.5 \times 10^4$ ml/g, remaining independent of total solution ionic strength as measured by dissolved-solids content.

At about 500 days since zero time, curves *A* and *B* of figure 14 approach each other, indicating approach to sorption equilibrium. The approximate time of 500 days for sorption equilibrium to be reached probably is longer than the time to equilibrium which would be observed in a system not disturbed by flow down the reentry hole. These data clearly show that instantaneous sorption equilibrium does not exist in explosion-cavity situations. A quantitative estimate of rate constants from the data is not possible, however.

Comparison of sample radioactivity values and their corresponding collection dates (days since zero time) with information contained in classified documents concerning the amounts and kinds of radioactivity expected to be produced by the Cannikin explosive confirm the presence of isotopes whose half-lives are similar to those calculated and used to produce curve *A* in figure 14. Thus, one may infer that the distribution of radioactivity in the aqueous phase is similar to the distribution of all radioactivity produced by the explosion. Although fractionation of certain isotopes and chemical forms must occur, it is apparently insufficient to cause large changes in the distribution of gross beta/gamma radioactivity that existed during the time interval after detonation considered in this study. At longer times after detonation, amounts and kinds of residual activity probably are controlled by selective sorption equilibria, and only loosely bound activities will remain in solution, but for intermediate times (250 to 550 days) no such selectivity is apparent. Studies now underway at older explosion sites should illuminate the question of ra-

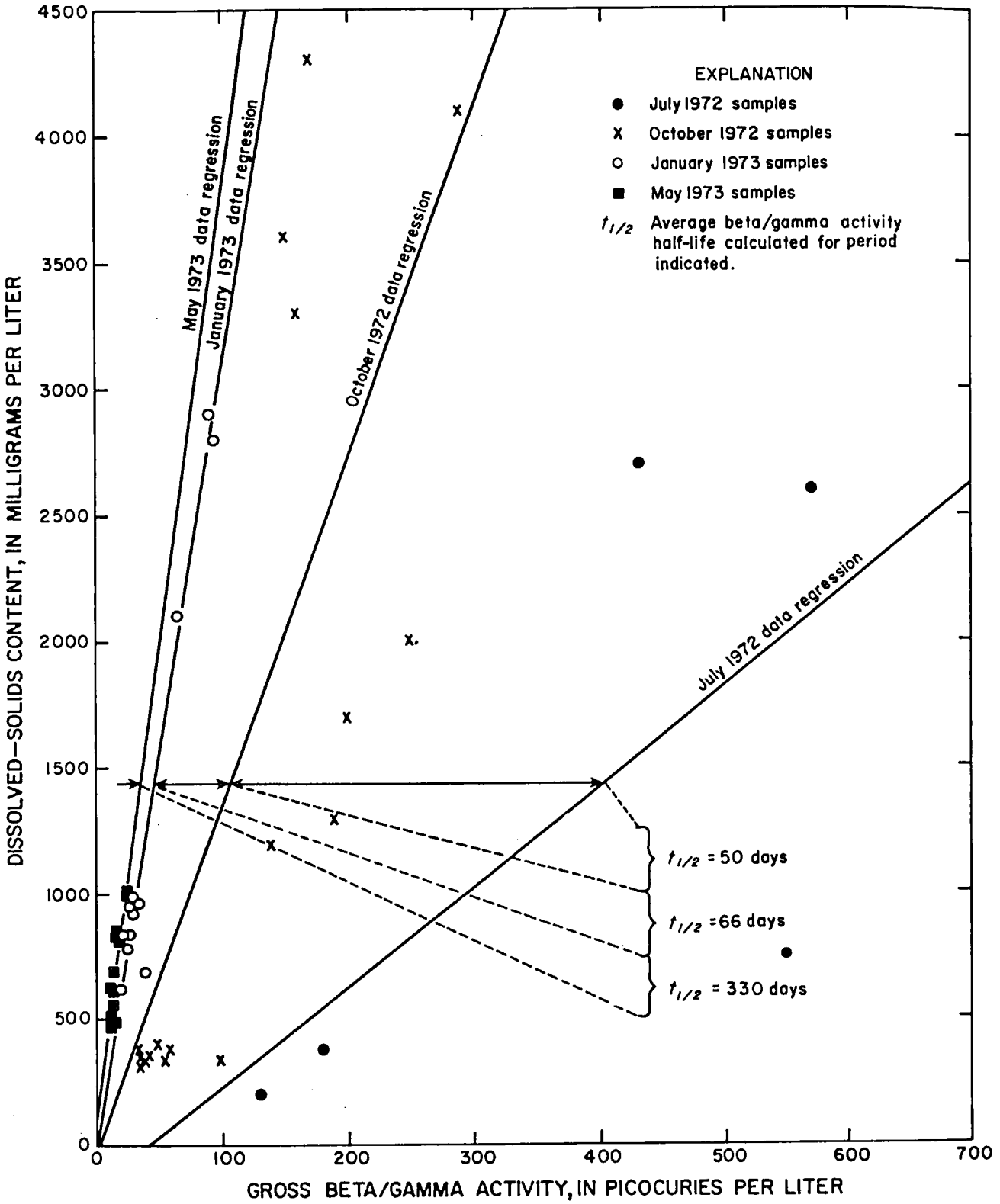

FIGURE 15. — Gross beta/gamma activity versus dissolved-solids content regression lines for the various sampling episodes in UA-1-P1 and determination of average radioisotope half-life.

dionuclide distribution in the aqueous phase at longer times.

TRITIUM ACTIVITY

As previously postulated, samples collected from UA–1–P1 represent mixtures of radioactive water of dissolved-solids content similar to that which filled the cavity (mainly from aquifer 3B) and nonradioactive low-dissolved-solids water which entered the cavity from near ground surface by downward flow in the vicinity of the drill hole. Because tritium values were not significantly affected by decay during the entire sampling period and because the above postulate leads to a linear relationship between dissolved solids and tritium concentration, a linear-regression analysis was performed on the tritium and dissolved-solids data. Not all analyses were used: samples collected from above the highest perforations (zone F) and samples collected prior to July 22, 1972, were omitted, the former because they likely did not represent water from outside the drill stem and the latter because some of the samples clearly indicate the presence of highly tritiated condensed steam from the cavity prior to the mixing induced by downward movement of water in the UA–1–P1 drill hole. Figure 12, introduced earlier, is a semilogarithmic plot of tritium versus dissolved solids. Inasmuch as a linear relationship is postulated, the reader might question the use of a semilogarithmic plot; it was necessitated by the four-order-of-magnitude range in tritium values. The best linear-fit regression line is also shown. A correlation coefficient of 0.73 for these data strengthens the simple-mixing postulate as reasonable. Some of the data scatter is a result of the reaction of the introduced fresh water with the rock matrix with which it comes in contact, as discussed earlier. This reaction causes higher dissolved-solids values for samples that have mixed in given proportion with the radioactive cavity water than would be predicted by simple mixing of two waters. This is particularly evident in the portion of figure 12 between 300 and 1000 mg/L dissolved solids and in the vicinity of 1×10^{-5} pCi/L tritium activity: the October 1972, January 1973, and May 1973 samples fall in the same dissolved-solids sequence as in figure 13 where their placement describes a reaction coordinate of surface water with subsurface rock.

The extrapolation of the tritium versus dissolved-solids content data to a dissolved-solids value of aquifer 3B (table 3) to determine radioactive-source water concentration in the cavity is tempting, but the assumption must be made that the cavity-fill water is completely homogeneous throughout. This assumption is probably not valid, as indicated by the radioactivity in the samples collected prior to July 22, 1972. Some of these samples presumably contain the condensed steam which apparently had not mixed with water from aquifer 3B in the 4 months that had elapsed from day of condensation to the day that water entered the drill stem. What did occur in the region of the cavity near the UA–1–P1 hole is mixing of water from aquifer 3B with water from near surface by strong local convection induced by the cool downward-moving current of water from near surface. Generalized cavitywide convection of any magnitude is not apparent from examination of the available data.

ALPHA ACTIVITY

Alpha activities, measured using natural uranium as a calibration standard, were either undetected or generally as low as those measured in the natural environment prior to Cannikin. There are a few notable exceptions which may be found in table 2. No identification of specific radionuclides was made on these samples and it is not known whether they represent alpha activity generated by the nuclear device or if present as a consequence of the large amounts of drilling fluid used in drilling UA–1–P1. These drilling fluids contained significant natural alpha activity in the form of uranium and thorium. Very small amounts of these fluids, if present in a sample, could account for the observed alpha activity.

Three of the samples in table 2, those collected on July 19, 22, and 23, 1972, were specifically analyzed for plutonium isotopes 239 and 240 and also for uranium 238 and 235 (Eric T. deJonckheere, Jr., written commun., 1975). No plutonium was detected, and the uranium-isotope ratio indicated natural uranium was present in the three samples.

CALCULATION OF CAVITY RADIUS FOR THE CANNIKIN EVENT

Although the exact energy yield of the Cannikin nuclear explosion, the measured radius of the lower hemisphere of the cavity, and the cavity void volume are not available because this is classified information, an approximate radius and void volume of the cavity can be established using published data on the effects of underground nuclear explosions (Butkovich and Lewis, 1973), and generalized information on the Cannikin event (Merritt, 1973). Thus, the radius and volume of the cavity formed by a nuclear explosion can be determined by the relationship

$$R_c = \frac{CW^{1/3}}{(\bar{\rho}\,h)^{\alpha}},$$

where R_c is the cavity radius of the lower hemisphere, in meters; W is the energy yield, in kilotons; $\bar{\rho}$ is the

average overburden density, in g/cm^3; and h is the depth of burst, in meters. The exponent α depends on the water content of the medium at the point of burst (Higgins and Butkovich, 1967), and C is a constant equal to about 100 using this set of units.

For the Cannikin event, stated to be a nuclear test of somewhat less than five megatons (Mt) yield, where:

W = 5000 kt (Merritt, 1973)
C = 100 (Butkovich and Lewis, 1973)
$\bar{\rho}$ = 2.3 g/cm^3 (Lee, 1969)
h = 1790 m (Merritt, 1973)
α = 0.307 (6.5 weight percent water) (Higgins and Butkovich, 1976; Lee and Gard, 1971)

Then,

for $W = 5000$ kt, $R_c = 133$ m.

SUMMARY AND CONCLUSIONS

The Cannikin nuclear explosive was detonated November 6, 1971, on Amchitka Island, Alaska, and an underground cavity was immediately created around the explosion. The stress placed on the overlying rock by the cavity was relieved by collapse of the overburden, creating a rubble chimney extending from the cavity to land surface. Increased vertical hydraulic conductivity over that which existed in the undisturbed environment resulted, and water from surface and subsurface sources flowed into and down the chimney to fill the new void created by the explosion. Water percolating toward the cavity region encountered an upward-moving front of high-temperature steam and water which severely retarded downward movement of water by two mechanisms — (1) vaporization of the downward percolating water, and (2) decreased hydraulic conductivity owing to two-phase flow conditions existing at the steam/water interface. Initially the interface moved upward; then, when sufficient cooling had occurred, it retreated downward.

During the downward flow retardation of water from surface and subsurface sources continued to accumulate in the chimney above the cavity. When the pressure and temperature conditions had allowed steam condensation to occur throughout much of the cavity, water which had accumulated in the chimney flowed downward, filling the cavity. Flow into the upper part of the chimney recommenced, and the progress of refilling the chimney was recorded by periodic water-level measurements in a reentry hole drilled into the Cannikin chimney and cavity.

The reentry-hole water levels represented combined measurements of water-vapor pressure in the cavity and hydraulic head in the chimney; consequently, to obtain true chimney water levels, the reentry-hole water levels were corrected for the effect of water vapor by using the estimated temperature history of the cavity. The water-level rise in the chimney thus obtained was combined with aquifer-property data, surface-water inflow, and an estimate of the magnitude of total new subsurface pore space created by the explosion to estimate the vertical distribution of new porosity within most of the chimney. Aquifer-property data had been obtained from a test hole near the Cannikin emplacement hole and surface-water inflow data were estimated from stream records obtained prior to detonation. Choice of day of steam condensation (day 60) and relative cavity radius of 1.34 (to obtain a corresponding subsurface void volume) were made to best fit the observed phenomena. The resulting calculated porosity distribution, which was in disagreement with published predictions, was 10 percent near the bottom of the chimney, decreasing to 4 percent near the top. As the magnitude of subsurface void is dependent on cavity size and shape, and therefore not known with certainty, calculations were made using several values of cavity radius. Furthermore, the water inflow was controlled by aquifer properties and the time that the chimney filling was renewed, immediately after steam condensation in the cavity. Therefore, different values for day of steam condensation in the cavity were paired with different values of cavity radius (directly related to magnitude of subsurface void) to determine the sensitivity of calculated porosity values to errors in estimating these parameters. It was found that a large error in estimate of magnitude of subsurface void (for example, 170 percent) results in a small relative error (45 percent) in porosity. The error introduced by an improper choice of day of steam condenstaion in the cavity is also small. The choice of $D_c = 60$ and $R_{rc} = 1.34$ as most probable was corroborated by calculations of distribution within the cavity of heat produced by the explosion.

In contrast to the hydraulic data, interpretation of the chemical information obtained from samples collected in the vicinity of Cannikin presented greater difficulty. The primary reason for this lay in the method of completion of the reentry hole and the techniques used in obtaining samples therefrom.

Downward flow of water from near land surface within and in the vicinity of the reentry hole was identified by temperature and FLO-PAK logs. Consideration of the water-quality data in light of this phenomenon made it possible to identify the effect of this near-surface water on the samples collected. Generally, the most radioactive samples approached a chemical composition similar to the native saline water near the cavity. The saline water was diluted by fresher water from near land surface. In addition to acting as a dilutant, the fresh water underwent changes in chemical

composition as it flowed downward, not unlike that which occurred in the undisturbed system prior to the detonation but much compressed in time. It is presumed that contributions of near-surface water to the overall chimney underwent similar changes. The concept of simple-mixing of two waters would theoretically allow calculation of radioactivity in undiluted cavity water; however, reaction of dilutant with aquifer matrix and the indication that water in the cavity region was not quantitatively (completely) mixed, contributed to data scatter that obviated precise extrapolation.

Indications from the general chemical data that quantitative mixing had not occurred in the cavity were corroborated by an analysis of the radiochemical data. Changes with time in radiochemical composition of the water samples indicated that even radiochemical equilibrium had not been achieved in the 18 months which had elapsed since detonation. This water-quality heterogeneity and consequent radioactive disequilibrium is perhaps not surprising, as it is difficult to postulate a mechanism for complete mixing to be rapidly attained. Large thermal gradients do not appear to have persisted in the Cannikin cavity. It is certainly possible that "hot spots" existed at time of abandonment of the site, but, if randomly distributed, they would contribute little to mixing of the cavity water. Thus, it is concluded that diffusion is the only process by which mixing would continue.

At the time of site abandonment, hydraulic equilibrium, as indicated by comparison of chimney water level with predetonation conditions, also had not been reached. This could be explained either by further cooling of the "hot spots" or by continued saturation of pore space of low hydraulic conductivity. With increased vertical hydraulic conductivity in the vicinity of Cannikin caused by chimney formation, a new hydraulic system could be formed which would result in deeper circulation of near-surface water than was previously possible. Because the more transmissive aquifers lie well above the cavity region, it is believed that this deepened circulation will not be significant below aquifers 1 or 2.

SELECTED REFERENCES

Ballance, W. C., 1970, Hydraulic tests in hole UA–1 and water inflow into an underground chamber, Amchitka Island, Alaska; U.S. Geol. Survey rept. USGS–474–72, 54 p.; available *only* from U.S. Dept. Commerce, Natl. Tech. Inf. Service, Springfield, Va. 22161.

_____1972, Hydraulic tests in hole UAE–1, Amchitka Island, Alaska: U.S. Geol. Survey rept. USGS–474–102, 32 p.; available *only* from U.S. Dept. Commerce, Natl. Tech. Inf. Service, Springfield, Va. 22161.

Beetem, W. A., Young, R. A., Washington, C. L., and Schroder, L. J., 1971, Chemical analyses of water samples collected on Amchitka Island, Alaska: U.S. Geol. Survey rept. USGS–474–135, 18 p.; available *only* from U.S. Dept. Commerce, Natl. Tech. Inf. Service, Springfield, Va. 22161.

Butkovich, T. R., and Lewis, A. E., 1973, Aids for estimating effects of underground nuclear explosions: Univ. California rept. UCRL–50929, Rev. 1, p. 7.

Carr, W. J., and Quinlivan, W. D., 1969, Progress report on the geology of Amchitka Island, Alaska: U.S. Geol. Survey rept. USGS–474–44, 15 p.; available *only* from U.S. Dept. Commerce, Natl. Tech. Inf. Service, Springfield, Va. 22161.

Dudley, W. W., Jr., 1970, Nonsteady inflow to a chamber within a thick aquitard: U.S. Geol. Survey Prof. Paper 700–C, p. C206–C211.

Fenske, P. R., 1972, Event-related hydrology and radionuclide transport at the Cannikin site, Amchitka Island, Alaska: U.S. Atomic Energy Comm., Nevada Operations Office rept. NVO–1253–1, 41 p.; available *only* from U.S. Dept. Commerce, Natl. Tech. Inf. Service, Springfield, Va. 22161.

Garber, M. S., 1971, A method for estimating effective porosity in a rubble chimney formed by an underground nuclear explosion: U.S. Geol. Survey Prof. Paper 750–C, p. C207–C209.

Gonzalez, D. D., and Wollitz, L. E., 1972, Hydrological effects of the Cannikin event: Seismol. Soc. America Bull., v. 62, no. 6, p. 1527–1542.

Gonzalez, D. D., Wollitz, L. E., and Brethauer, G. E., 1974, Bathymetry of Cannikin Lake, Amchitka Island, Alaska, with an evaluation of computer mapping techniques: U.S. Geol. Survey rept. USGS–474–203, 20 p.; available *only* from U.S. Dept. Commerce, Natl. Tech. Inf. Service, Springfield, Va. 22161.

Hantush, M. S., 1959, Nonsteady flow to flowing wells in leaky aquifers: Jour. Geophys. Research, v. 64, no. 8, p. 1043–1052.

Heckman, R. A., 1964, Deposition of thermal energy by nuclear explosives, *in* Engineering with nuclear explosives: Third Plowshare Symposium Proc., U.S. Atomic Energy Comm. Rept. TID–7695, p. 259–304.

Higgins, G. H., and Butkovich, T. R., 1967, Effect of water content, yield, medium, and depth of burst on cavity radii: Univ. California rept. UCRL–50203, 24 p.

Hodgman, C. D., ed., 1957, Handbook of chemistry and physics, 39th ed.: Cleveland, Ohio, Chem. Rubber Publishing Co., 3213 p.

Lee, W. H., 1969, Some physical properties of rocks in drill hole UAE–1, Amchitka Island, Alaska: U.S. Geol. Survey rept. USGS–474–48, 13 p.; available *only* from U.S. Dept. Commerce, Natl. Tech. Inf. Service, Springfield, Va. 22161.

Lee, W. H., and Gard, L. M., Jr., 1971, Summary of the subsurface geology of the Cannikin site, Amchitka Island, Alaska: U.S. Geol. Survey rept. USGS–474–132, 24 p.; available *only* from U.S. Dept. Commerce, Natl. Tech. Inf. Service, Springfield, Va. 22161.

Merritt, M. L., 1973, Physical and biological effects of Cannikin, U.S. Atomic Energy Commission rept. NVO–123, 106 p.

Morris, R. H., 1973, Topographic and isobase maps of Cannikin sink: U.S. Geol. Survey rept. USGS–474–125, 8 p.; available *only* from U.S. Dept. Commerce, Natl. Tech. Inf. Service, Springfield, Va. 22161.

Pirson, S. J., 1958, Oil Reservoir Engineering, 2d ed.: New York, N.Y., McGraw-Hill Book Co., 733 p.

Schroder, L. J., and Ballance, W. C., 1973, Summary of chemical and radiochemical monitoring of water for the Cannikin event, Amchitka Island, Alaska, fiscal year 1972: U.S. Geol. Survey rept. USGS–474–167, 39 p.; available *only* from U.S. Dept. Commerce, Natl. Tech. Inf. Service, Springfield, Va. 22161.

★U.S. Government Printing Office: 1977-777-102/17